Author Manuscript

Author Manuscript

Author Manuscript

Author Manuscript

HHS Public Access

Author manuscript

Sci Signal. Author manuscript; available in PMC 2021 May 25.

Published in final edited form as:

Sci Signal. ; 11(528): . doi:10.1126/scisignal.aai9085.

Nuclear PTEN enhances the maturation of a microRNA regulon to limit MyD88-dependent susceptibility to sepsis

Flavia Sisti[#1], **Soujuan Wang**[#1], **Stephanie L. Brandt**[#1,2], **Nicole Glosson-Byers**[1], **Lindsey Mayo**[3], **Young min Son**[1], **Sarah Sturgeon**[2], **Luciano Filgueiras**[1,4], **Sonia Jancar**[4], **Hector Wong**[5], **Charles S. Dela Cruz**[6], **Nathaniel Andrews**[6], **Jose Carlos Alves-Filho**[7], **Fernando Q. Cunha**[7], **C. Henrique Serezani**[1,2,*]

[1]Department of Microbiology and Immunology, Indiana University School of Medicine, Indianapolis, IN, USA. ZIP 46202

[2]Division of Infectious Diseases, Department of Medicine, Vanderbilt University Medical Center, Nashville, TN, USA. ZIP 37232

[3]Herman B Wells Center for Pediatric Research Departments of Pediatrics and Biochemistry and Molecular Biology, Indiana University School of Medicine, Indianapolis, IN, USA. ZIP 46202

[4]Department of Immunology, Institute of Biomedical Sciences, University of Sao Paulo, Sao Paulo, Brazil. ZIP 05508-000

[5]Division of Critical Care Medicine, Cincinnati Children's Hospital Medical Center and Cincinnati Children's Hospital Research Foundation, Cincinnati, Ohio, USA. ZIP 45229-3026

[6]Section of Pulmonary and Critical Care Medicine, Department of Internal Medicine, Yale University School of Medicine, New Haven, CT, USA. ZIP 06520

[7]Department of Pharmacology, Ribeirao Preto Medical School, University of Sao Paulo, Ribeirao Preto, Brazil. 14049-900

[#] These authors contributed equally to this work.

Abstract

Sepsis-induced organ damage is caused by systemic inflammatory response syndrome (SIRS), which results in substantial comorbidities. Therefore, it is of medical importance to identify molecular brakes that can be exploited to dampen inflammation and prevent SIRS development. The current study investigated the role of phosphatase and tensin homolog (PTEN) in suppressing SIRS, increasing microbial clearance, and preventing lung damage. Septic patients and mice with sepsis exhibited increased *PTEN* expression in leukocytes. Myeloid-specific *Pten* deletion

[*]Address correspondence: Vanderbilt University Medical Center, Division of Infectious Disease, Department of Medicine, Nashville, TN, USA. 1161 21st Avenue South, Suite A2310A, MCN, Nashville, TN, 37232. Tel +1(615) 875-8626. h.serezan@vanderbilt.edu.

Author Contributions: Conceptualized and designed experiments: Sisti, F., Mayo, L., Alves-Filho, JC., Filgueiras L., Serezani, CH, Brandt, S, Glosson-Byers, N. Performed experiments: Sisti, F., Son, YM., Brandt, S., Wang, S., Sturgeon, S., Glosson-Byers, N., Dela Cruz, C A., Filgueiras, L., Andrews, N. Data analyses: Sisti, F., Mayo, L., Alves-Filho, JC, Filgueiras L., Serezani, CH, Brandt, S Glosson-Byers, N., Dela Cruz, C., Wong, H., Jancar S., Cunha F.Q. Manuscript preparation: Glosson-Byers, N and Serezani, C.H.

Competing interests: The authors have no conflicts of interest.

Data and materials availability: All data needed to evaluate the conclusions in the paper are present in the paper or the Supplementary Materials.

Author Manuscript Author Manuscript Author Manuscript Author Manuscript

increased bacterial loads and cytokine production, which depended on enhanced myeloid differentiation primary response gene 88 (MyD88) abundance and resulted in mortality in an animal model of sepsis. PTEN-mediated induction of the microRNAs miR-125b and miR203b reduced the abundance of MyD88. Loss- and gain-of-function assays demonstrated that PTEN drives microRNA production by associating and facilitating the nuclear localization of Drosha-Dgcr8, part of the microRNA processing complex. Introduction of a mutant form of PTEN that does not localize to the nucleus in PTEN-deficient mouse embryonic fibroblasts resulted in retention of Drosha-Dgcr8 in the cytoplasm and impaired production of mature microRNAs. Thus, we identified a regulatory pathway involving nuclear PTEN-mediated microRNA generation that limits production of MyD88 and thereby limits sepsis-associated mortality.

One Sentence Summary:

By limiting the innate immune response, nuclear PTEN prevents sepsis-induced organ damage.

INTRODUCTION

Dysregulated inflammatory responses contribute to many pathological conditions, including sepsis (1). Inflammatory response during sepsis is initiated by the activation of Toll-like receptor (TLR) and cytokine signaling in resident cells (2). In addition to sensing microbial products, the TLR pattern recognition receptors (PRRs) are activated by endogenous danger signals produced during tissue injury (2). Systemic inflammatory response syndrome (SIRS), characterized by uncontrolled production of inflammatory mediators, is the main cause of sepsis-induced multiple organ dysfunction (1). The resulting tissue injury depends the TLRs and cytokine receptors that initiate inflammatory pathways.

Activation and inactivation of an inflammatory response requires regulation and coordination among numerous receptors, signaling pathways, and mediators. TLR family members and the interleukin (IL)-1 receptor (IL-1R) share a conserved cytoplasmic Toll–IL-1R (TIR) domain that recruits adaptor proteins, including myeloid differentiation factor 88 (MyD88), upon stimulation. MyD88 is a central adaptor protein that mediates signaling through all of the known TLRs except TLR3 (2). MyD88 is essential for cytokine induction after stimulation with various ligands, such as cytokines (IL-1β and IL-18), danger-associated molecular patterns (DAMPs), and microbial pathogen-associated molecular patterns (PAMPs) (3). MyD88 deficiency increases susceptibility to a broad range of pathogens and inflammatory diseases (4). Expression of the gene encoding *Myd88* is augmented by proinflammatory mediators (5) and is regulated at multiple levels, including transcription (6) and translation by microRNAs (7, 8). microRNAs are small endogenous RNA molecules, ~22 nucleotides in length, that regulate gene expression by targeting mRNAs for translational repression or degradation (9). Five miRNAs—miR125b, miR200b, miR200c, miR203, and miR155—inhibit MyD88 actions and TLR responsiveness (7, 8, 10, 11). Given the complexity of signaling and regulation involved in an inflammatory response, identifying molecular brakes with pleiotropic actions could potentially prevent the development of SIRS and organ damage by dampening harmful levels of inflammation.

Author Manuscript Author Manuscript Author Manuscript Author Manuscript

Phosphatases prevent aberrant cellular activation by limiting the propagation of kinase signaling cascades and controlling transcriptional networks. The tumor suppressor, phosphatase and tensin homolog (PTEN), is a lipid and protein phosphatase with widespread actions. The PTEN lipid phosphatase catalytic site is conventionally known to dephosphorylate PIP3, a product of phosphoinositol-3-kinase (PI3K), which is required for the activation of protein kinase B (PKB, also known as Akt), a kinase that protects various cell types against apoptosis (12). The PTEN protein phosphatase catalytic site is less well characterized but has been proposed to regulate nuclear functions through facilitating transcription factors binding to promoter sequences and maintenance of chromosomal integrity (13).

There is controversy concerning the role of PTEN in regulating the actions of TIR adaptors. Whereas macrophages from both PTEN heterozygous mice and mice specifically deficient in myeloid cell PTEN are less responsive to TLR4 or TLR5 ligands (14, 15), pharmacological inhibition of PTEN enhances TLR-mediated cytokine production (16). In addition, myeloid-specific PTEN deficiency leads to increased susceptibility to lung infection by Gram-negative and -positive bacteria (17, 18). Further, macrophages from global PTEN −/+ mice exhibit lower LPS-induced TLR4 membrane translocation compared to WT macrophages (19). PTEN is also a negative regulator of IL-1R signaling, through inhibition of nuclear factor kappa-light-chain-enhancer of activated B cells (NF-κB), a transcription factor that mediates the inflammatory response (20). PTEN also impairs the killing and phagocytosis of non-opsonized bacteria and the yeast *Candida albicans* (18, 21).

Because PTEN is a pleiotropic molecule that regulates various pathways of the immune response, it may be a useful target for therapeutic intervention during sepsis. PTEN activation could lead to impairment of both IL-1R and TLR signaling and improve the outcome of SIRS. Although PTEN might represent an attractive target in the early stages of sepsis, where a molecular brake is needed to dampen the inflammatory response, constitutive PTEN activation might lead to impairment in macrophage function, as observed in septic patients (22). In the current study, we investigated the role of PTEN in controlling the microRNA-mediated macrophage inflammatory response during sepsis, with the goal of identifying molecular pathways involved in this excessive inflammatory response.

RESULTS

PTEN inhibition drives mortality and increases lung injury in septic mice.

Initially, we determined whether *PTEN* mRNA abundance changed during sepsis in both humans and mice. Peritoneal cells from mice undergoing polymicrobial sepsis induced by cecal ligation and puncture (CLP) had increased *Pten* mRNA abundance compared to cells from sham-treated mice (Fig. 1A). *PTEN* mRNA increased in blood leukocytes of adult septic patients who died (expired) compared to patients who survived (Fig. 1B). An increase also occurred in pediatric patients that had septic shock compared to healthy controls (Fig. 1C), and *PTEN* abundance was less in pediatric septic patients that survived and developed severe comorbidities associated with sepsis (endotype A), compared to septic children that did not develop comorbidities (endotype B) (Fig. 1D).

Author Manuscript Author Manuscript Author Manuscript Author Manuscript

To study if PTEN influenced the outcome of sepsis, we inhibited PTEN *in vivo* with the PTEN inhibitor Bpvic(OH) or knocked down PTEN expression with specific siRNAs prior to inducing CLP-mediated sepsis in mice. PTEN inhibition significantly reduced animal survival (Fig. 2A). This effect was associated with increased bacterial burden in peritoneal exudates 24 hours after CLP in comparison to control CLP mice administered either vehicle or scrambled siRNA (Fig. 2B). In addition, the numbers of neutrophils increased in the peritoneal cavity of CLP mice compared to sham-operated mice (Fig. 2C), whereas inhibition of PTEN with Bpvic(OH) or siRNA knockdown resulted in reduced numbers of neutrophils in the peritoneal cavity after CLP (Fig. 2C and D). However, production of cytokines in peritoneal exudates 24 hours after CLP increased, including an increase in IL-1β, TNFα, and IL-6, in PTEN-knockdown CLP mice in comparison to CLP mice received scrambled siRNA (Fig. 2E).

Monocytes, macrophages, and neutrophils play a critical role in the pathogenesis of sepsis (23). We therefore utilized the Cre-Lox recombination system to cross $PTEN^{fl/fl}$ and $LysM^{cre}$ mice, generating mice deficient in PTEN specifically in myeloid cells. Myeloid-specific PTEN deletion increased mortality of septic mice (Fig. 2F), which correlated with increased TNFα, IL-1β, and IL-6 abundance in serum and the peritoneal cavity (Fig 2G). To determine whether the increased bacterial load mediates organ injury, we administered antibiotic (ertapenem) to PTEN inhibitor-treated mice 1 hour after the induction of sepsis and then twice a day for 3 days. Although antibiotic treatment restored survival in septic mice treated with the vehicle control, the mice administered the PTEN inhibitor and antibiotic showed decreased survival, indicating that loss of PTEN function drives inflammation-mediated organ damage and mortality in septic mice (fig. S1)

Next, we determined whether PTEN was protective during peritonitis induced by methicillin-resistant *Staphylococcus aureus* (MRSA) (24). Mice were treated with PTEN inhibitor or vehicle control 24 hours before MRSA intraperitoneal infection. PTEN inhibition resulted in reduced survival and significantly increased bacterial burden in the peritoneal exudates 24 hours after MRSA infection (fig. S2A and B). This was accompanied by enhanced TNFα production in the serum and peritoneal cavity (fig. S2C). Together, these data showed that PTEN prevents an uncontrolled host defense response to infection and SIRS development, improving survival in two different models of sepsis.

Systemic infection induced by sepsis can affect a number of organs, including the lung (25). Therefore, we analyzed PTEN abundance in lung sections and total lung homogenates 24 hours after CLP. Confocal microscopic analysis of lung sections showed that PTEN abundance increased in macrophages and bronchial epithelial cells following CLP (fig. S3A). In addition, *Pten* mRNA abundance increased in total lung homogenates (fig. S3B).

To determine if PTEN inhibition resulted in increased inflammation in the lung during sepsis, mice were treated with control or PTEN siRNA prior to receiving CLP, and 24 hours later, bronchoalveolar lavage (BAL) and whole lung were isolated. PTEN inhibition was accompanied by increased cell recruitment into the lungs, visualized in hematoxylin and eosin (H&E)-stained lung sections (fig. S3C). Although alveolar edema and capillary congestion, two measurements of pulmonary inflammation, were increased in CLP mice

Author Manuscript Author Manuscript Author Manuscript Author Manuscript

receiving scrambled siRNA, CLP mice with siRNA targeting PTEN had significantly increased amounts of these indicators of pulmonary inflammation (fig. S3D and E). PTEN knockdown was also accompanied by increased abundance of the proinflammatory cytokines IL-1β and TNFα in the BAL of CLP mice (fig. S3F). These data suggested that PTEN represses lung inflammation induced during polymicrobial sepsis.

Silencing PTEN increases MyD88 abundance and macrophage responsiveness.

Phagocytes play a significant role in the control of bacterial clearance and inflammatory response. While macrophages are required for the development of SIRS, neutrophils are key in controlling bacterial growth. Given that lack of PTEN increased immune cell cytokine production, decreased neutrophil numbers at the site of infection, along with data shown in the fig. S1 demonstrating that antibiotic treatment does not prevent enhanced mortality in PTEN inhibitor-treated septic mice, we anticipated that the role of PTEN in SIRS development would be restricted to macrophages. Therefore, we investigated the molecular pathways involved in increased cytokine production in myeloid-specific PTEN-deficient mice during sepsis. Specifically, we examined the role of PTEN in macrophage activation using thioglycollate-elicited peritoneal macrophages as a model of inflammatory cells. Macrophages were transfected with siPTEN or scrambled siRNA control, followed by treatment with lipopolysaccharide (LPS), a TLR4 ligand that uses both MyD88 and TRIF adaptors; Pam3CSK4, a TLR2 ligand that depends on MyD88 activity; or polyinosinic-polycytidylic acid [Poly(I:C)], a TLR3 ligand that signals exclusively through TRIF (26). In PTEN-silenced macrophages, LPS and Pam3CSK4, but not Poly(I:C), induced increased NF-κB p65 phosphorylation compared to siRNA control macrophages (Fig. 3A). In addition, LPS induced increased nitrite production in PTEN-silenced cells compared to siRNA control cells (Fig. 3B). Further ruling out a role for PTEN in macrophage activation by TRIF-mediated TLR3 signaling, we found that PTEN deficiency did not influence LPS or Poly(I:C)-mediated interferon regulatory factor (IRF)3 phosphorylation (fig. S4A), a transcription factor involved in TRIF-dependent gene transcription (27). In addition, PTEN deficiency did not affect the production of TRIF-dependent cytokine interferon (IFN)-β and chemokine CXCL10 (fig. S4B, C).

Interleukin-1 receptor-associated kinase (IRAK)-4 and IKKα are kinases that are downstream of MyD88 (28, 29). To determine if PTEN directly dephosphorylated IRAK-4 and IKKα, we performed an in-blot PTEN activity assay. Lysates from macrophages challenged with LPS, peptidoglycan (PGN), curdlan (a dectin-1 ligand), or Poly(I:C) for 30 min were transferred to membranes and then incubated with buffer alone, recombinant PTEN, or the positive control alkaline phosphatase. Membranes were probed for phosphorylated IRAK-4 or IKKα. Membranes treated with buffer or recombinant PTEN yielded a prominent band for phosphorylated IRAK-4 and IKKα in response to LPS (fig. S5). The phosphorylated proteins were undetectable in the alkaline phosphatase-treated membranes. When membranes were stripped and re-probed for actin, there was no observed difference among the treatment groups, excluding a role for PTEN protease activity. These data suggested that PTEN inhibits MyD88-dependent signaling through an effect on MyD88, rather than downstream effects on kinases involved in NF-κB activation.

Author Manuscript Author Manuscript Author Manuscript Author Manuscript

To determine if PTEN altered the abundance of TLR4 and TIR adaptor abundance, we compared the abundance of various adaptors and TLR4 in macrophages with scrambled siRNA or PTEN-targeted siRNA. PTEN-silenced macrophages had increased abundance of MyD88 but not of TLR4 or other adaptors, compared to siRNA control macrophages (Fig. 3C). Peritoneal cells from mice treated in vivo with siRNA targeting PTEN or $PTEN^{flf/fl}$_$LysM^{cre}$ had increased MyD88 abundance in comparison to cells from control siRNA-treated or $PTEN^{fl/fl}$ mice (Fig. 3D and E). Furthermore, the LPS induced increase in MyD88 in macrophages from mice in which PTEN was deleted ($PTEN^{flf/fl}$_$LysM^{cre}$ mice) was greater than that in cells from wild-type ($PTEN^{fl/fl}$) mice (Fig. 3E). We confirmed that PTEN reduced *Myd88* mRNA abundance in macrophages transduced with active PTEN-expressing adenovirus (fig. S6A and B). In transduction experiments with adenovirus expressing active PTEN, or adenovirus expressing PTEN lacking lipid phosphatase activity (G129E mutant), or adenovirus expressing a dominant-negative form of PTEN that lacks both protein and lipid phosphatase activity (C214S mutant), we found that MyD88 protein abundance was undetectable in cells expressing active PTEN and was substantially reduced in cells expressing the G129E mutant (fig. S6C). Therefore, these results indicated that PTEN lipid phosphatase activity inhibits the production of MyD88. Together, the data in Figure 3 and in figure S6 indicated that the lipid phosphatase activity of PTEN limits homeostatic and inducible MyD88 production and inhibits TLR and IL-1R signaling in macrophages.

Increased MyD88 in PTEN-deficient mice enhances mortality during sepsis.

To further test our hypothesis that increased susceptibility to sepsis in PTEN-deficient mice depended on increased MyD88 abundance, we measured *Myd88* mRNA in peritoneal cells from septic mice treated with the PTEN inhibitor. *Myd88* mRNA abundance was decreased 24 hours after sepsis and PTEN inhibition not only reversed this effect, but the expression in the *Myd88* mRNA exceeded that of the sham-operated mice (Fig. 4A). We performed rescue experiments to determine if blocking MyD88 could overcome the enhanced mortality observed in PTEN-silenced mice. Administration of a MyD88 blocking peptide 1 hour after CLP significantly improved survival of PTEN-silenced mice (Fig. 4B), which was accompanied by decreased bacterial burden (Fig. 4C) and reduced proinflammatory cytokine production (Fig. 4D). We confirmed the specificity of the MyD88 blocking peptide in macrophages stimulated with LPS, PAM3CSK4, or Poly(I:C). Whereas all these agonists induced nitrite (a nitric oxide metabolite) production, the MyD88 blocking peptide inhibited TLR4 and TLR2 but not TLR3 signaling, demonstrating the specificity of the peptide in blocking MyD88 action (fig. S7). These data point to a PTEN-MyD88 axis that controls inappropriate inflammation in polymicrobial sepsis. Further, these results demonstrate an epistatic relationship between PTEN and MyD88, promoting a signaling balance to maintain homeostatic inflammatory responses during pathogen challenge.

PTEN regulates MyD88 expression in macrophages.

Myd88 expression and protein production are controlled at multiple levels, including STAT1 and NF-κB activation (6) and mRNA degradation by specific microRNAs (8, 10). To determine if PTEN regulated *MyD88* expression through an effect on STAT1, we determined STAT1 abundance and activation, measured as STAT1 phosphorylation on serine

Author Manuscript Author Manuscript Author Manuscript Author Manuscript

727 or tyrosine 701, in PTEN-knockdown or siRNA control macrophages. We did not detect any change in total or phosphorylated STAT1 with in PTEN-silenced cells compared to control siRNA cells (fig. S8A). When alveolar macrophages were transduced with adenovirus expressing active PTEN, dominant-negative PTEN (C124S), or lipid phosphatase-deficient PTEN (G129E), we saw no effect on STAT1 abundance or tyrosine 701 phosphorylation. However, overexpression of active PTEN inhibited phosphorylation of STAT1 on serine 727 in a manner that was independent of lipid phosphatase activity (fig. S8B).

We confirmed the lack of involvement of PTEN in STAT1 activation by showing that PTEN-deficient macrophages from the $PTEN^{flf/fl}$_$LysM^{cre}$ mice produced similar amounts of the STAT1-dependent chemokine CXCL1 in response to either LPS or Poly(I:C) (fig. S8C). To test the possibility that PTEN inhibited *Myd88* expression by controlling the activity of other transcription factors involved in *Myd88* expression, such as NF-κB and STAT3, we compared macrophages in which PTEN was knocked down or to siRNA control macrophages and that had been treated with the JAK2 inhibitor AG490 (6), the NF-κB inhibitor a p65 blocking peptide (30), or the STAT3 peptide inhibitor STATTIC (31). Inhibition of these transcription factors did not influence PTEN-mediated effects on *Myd88* mRNA abundance in macrophages (fig. S8D). These results suggested that microRNAs were involved in PTEN-mediated regulation of MyD88 abundance in macrophages.

Therefore, we evaluated the abundance of known inflammatory mature microRNAs, using an immunopathology focused array (10), in peritoneal macrophages treated with siRNA targeting PTEN or scrambled siRNA. Of 88 transcripts analyzed, 30 mature microRNAs were decreased in PTEN-silenced cells, including miR19a and miR19b, miR21, miR125a and miR12b, miR146a and miR146b, and miR203 (Fig. 5A), all of which have been reported to regulate TLR signaling (10, 32). In addition, 10 microRNAs known to regulate TLR responses (33–36) were enhanced in PTEN-silenced cells, including let7g and miR155 (Fig. 5A). The remaining 48 microRNAs tested did not change expression. We verified the abundance of individual microRNAs in PTEN-silenced peritoneal cells by qPCR (Fig. 5B). In addition, macrophages from naïve mice transduced with an adenovirus expressing constitutively active PTEN displayed increased miR125b and miR146b and decreased miR155 in comparison to cells transduced with control adenovirus (Fig. 5C).

To determine if PTEN regulated the abundance of microRNAs in myeloid cells *in vivo* and to confirm the siRNA findings, we analyzed the abundance of mature microRNAs in peritoneal macrophages from $PTEN^{fl/fl}$ or $PTEN^{fl/fl}$_$LysM^{cre}$ mice. The abundance of miR125b, miR19a, and miR146b in peritoneal cells from PTEN-deficient mice was reduced, whereas there was no change in the abundance of miR134 (Fig. 5D). We observed a similar effect on the abundance of miR125b, miR19a, and miR134 alveolar macrophages from $PTEN^{fl/fl}$_$LysM^{cre}$ mice (fig. S9). Examining PTEN-controlled microRNA abundance during sepsis showed that miR125a and b, miR181a, and miR21 abundance increased after CLP in wild-type mice and that PTEN deficiency prevented microRNA production in both sham and CLP groups (Fig. 5E). These data showed that PTEN regulates microRNA production during basal and inflammatory conditions.

Author Manuscript Author Manuscript Author Manuscript Author Manuscript

The PTEN lipid phosphatase domain controls signaling through the PI3K/Akt pathway (12). Akt controls activation of mammalian target of rapamycin (mTOR), which is crucial for many cell processes, including mRNA translation, *de novo* nucleotide synthesis, and autophagy (12). To investigate if the effects of PTEN on microRNA abundance depended on PI3K or mTOR activation, macrophages from PTEN$^{fl/fl}$ and PTEN$^{fl/fl}$_LysM^{cre} mice were treated with the PI3K inhibitor wortmannin or the mTOR inhibitor rapamycin. In wild-type cells, rapamycin but not wortmannin inhibited the production of miR125b (Fig. 5F), miR21, and miR203 (fig. S10A and B), indicating a role for mTOR in regulating basal microRNA production. However, only PI3K inhibition prevented the reduction in miR203 abundance in PTEN$^{fl/fl}$_LysM^{cre} macrophages, showing that the influence of PTEN on the production of this microRNA depended on its lipid phosphatase activity (fig. S10A). In contrast, PI3K inhibition by wortmannin did not rescue miR21 abundance in PTEN$^{fl/fl}$_LysM^{cre} cells, indicating a role for PTEN in controlling this micorRNA that is independent of the lipid phosphatase activity (fig. S10B).

We further analyzed changes in microRNA abundance to evaluate if they accounted for enhanced *Myd88* mRNA abundance and MyD88-mediated enhancement of macrophage activation in PTEN-silenced cells. Macrophages were transfected with siRNA against PTEN or scrambled control siRNA for 48 h, followed by transfection with the microRNA mimics miR155, miR125b and miR203 that were previously shown to be modulated by PTEN silencing for 24 h. *Myd88* mRNA abundance was then analyzed by qPCR. Although the miR155 and miR146b mimics had no effect on PTEN-mediated inhibition of *Myd88* mRNA abundance, miR125b and miR203 decreased *Myd88* mRNA only in PTEN-silenced cells (Fig. 5G). Confirming that miR125b and miR203 directly controlled *Myd88* expression, reduced expression of a luciferase reporter with the 3'UTR of *Myd88* was observed in the macrophage cell line transfected with miR125b and miR203 alone and introduction of both microRNAs further reduced expression (fig. S11A). In addition, *Myd88* transcripts coprecipitated with Ago2, a member of the RNA-induced silencing complex (RISC), in macrophages transfected with miR125b or miR203 mimics (fig. S11B).

Mimics of miR125b or miR203 also prevented the enhanced LPS-induced nitrite production in PTEN-silenced macrophages, an effect that was enhanced by combining both mimics (Fig. 5H). Together, these results indicated a previously unknown role for PTEN lipid phosphatase activity with both homeostatic and inducible production of microRNAs involved in macrophage *Myd88* expression and TLR signaling.

Nuclear PTEN regulates microRNA maturation.

microRNA abundance is regulated at numerous levels, including transcription, processing, and subcellular localization (37). To determine whether PTEN localization and the lipid phosphatase domain regulates microRNA production, we transfected HEK293 cells with lentiviral vectors expressing the following PTEN constructs: (i) C124S, a dominant-negative PTEN construct (21); (ii) G129E, a construct lacking lipid phosphatase activity (21); (iii) K163R, a construct lacking an acetylation site important for PTEN membrane translocation (38); (iv) K254R, a construct that cannot localize to the nucleus (39); and (v) K289R, a construct that exhibits reduced nuclear PTEN (40). The expression of these constructs in

Author Manuscript Author Manuscript Author Manuscript Author Manuscript

HEK293 cells were confirmed by immunoblotting (fig. S12). Active PTEN increased the abundance of miR125b and miR21 and decreased the abundance of miR155 (Fig. 6A). PTEN lacking lipid phosphatase activity (G129E) did not affect the abundance of these microRNAs, and the K254R and K289R mutant forms of PTEN, which cannot localize properly to the nucleus, did not alter the abundance of miR125b, miR155, or miR21 (Fig. 6A). These data indicated that nuclear localization of PTEN and its lipid phosphatase activity are necessary for microRNA processing.

Because PTEN regulated nuclear microRNA production, we investigated if PTEN influenced the abundance of the enzymes involved in microRNA maturation, such as Drosha and Dgcr88 (proteins involved in the generation of precursor microRNA), Xpo5 (Exportin 5, a protein that transports precursor microRNAs to the cytoplasm), and Dicer (the enzyme that generates mature microRNA) (41). We observed a similar mRNA expression of these genes in PTEN-deficient or wild-type macrophages (Fig. 6B). Next, we studied if PTEN controlled the expression of primary microRNAs (several hundred nucleotide-long RNA that will generate precursor miRNA) in macrophages lacking PTEN or in wild-type macrophages treated with siRNA targeting PTEN or scrambled siRNA. PTEN deficiency increased the expression of primary microRNAs for miRNA125b, miRNA155, miRNA203, Let-7e, and Let-7d (Fig. 6C and D), demonstrating that PTEN participates in the maturation of microRNAs.

Next, we determined if PTEN interacted with Drosha and Dgcr8 in macrophages, imaging was performed. Confocal microscopic analysis of macrophages from wild-type mice revealed nuclear and cytoplasmic colocalization of PTEN with Drosha and Dgcr8 (Fig. 6E). However, PTEN did not colocalize with Dicer in the cytoplasm of macrophages (Fig. 6E). Proximity ligation assay (PLA) confirmed that PTEN physically associated with Drosha and Dgcr8 in the nucleus of unstimulated macrophages from wild-type ($PTEN^{fl/fl}$) mice but not in macrophages from $PTEN^{fl/fl}$_$LysM^{cre}$ (Fig. 6F). PTEN, Drosha, and Dgcr8 coimmunoprecipitated from macrophage lysates, confirming the microscopy results (Fig. 6G). These results suggested that PTEN controls the nuclear translocation of Drosha and Dgcr8.

Therefore, we examined the localization of Drosha and Dgcr8 in macrophages from both $PTEN^{fl/fl}$ and $PTEN^{fl/fl}$_$LysM^{cre}$ mice. Dicer was located in the cytoplasm, but Drosha and Dgcr8 were localized mainly in the nucleus of wild-type macrophages. PTEN deficiency ($PTEN^{fl/fl}$_$LysM^{cre}$ mice) impaired Drosha and Dgcr8 nuclear localization without affecting the subcellular distribution of Dicer as evidenced by confocal microscopy (Fig. 6H) and by cellular fractionation of cytosolic and nuclear proteins (Fig. 6I). In all, these data indicate a role for PTEN in microRNA processing by directly regulating the distribution of microRNA processing enzymes in the nucleus.

DISCUSSION

Using a wide variety of cellular, molecular, genetic, and pharmacologic approaches, we identified a novel role for PTEN in regulating nuclear microRNA maturation, which plays important rolesin host innate immunity and decreased mortality and comorbidities

Author Manuscript Author Manuscript Author Manuscript Author Manuscript

associated with sepsis. In summary, our results demonstrated that 1) 1) *Pten* mRNA expression is enhanced in murine sepsis and in the blood of pediatric and expired adult septic patients. Furthermore, in septic patients that developed severe co-morbidites, PTEN expression is greatly decreased. 2) Genetic and pharmacologic inhibition of PTEN resulted in animal mortality during sepsis, accompanied by increased bacterial load, inflammatory cytokine production and lung injury. 3) PTEN deficiency led to exaggerated MyD88 abundance, and blocking MyD88 effects in PTEN-null mice prevented increased mortality and inflammatory responses during sepsis; 4) PTEN actions on MyD88 is due to the increased expression of microRNAs involved in macrophage activation in both naïve and septic mice; 5) PTEN lipid phosphatase activity and nuclear localization regulated microRNA expression; and 6) PTEN associated with and permitted nuclear translocation of Drosha and Dgcr8. In total, our data identified novel mechanisms by which the PTEN tumor suppressor regulates microRNAs, affecting macrophage activation and improving sepsis outcomes.

Sepsis is characterized by early development of SIRS, which leads to organ damage (1). Therefore, it is important to identify molecular pathways that prevent the development of SIRS and inhibit organ damage induced during sepsis. We observed that *PTEN* expression was increased during sepsis, which could suggest a regulatory role for PTEN in preventing overwhelming inflammation, mediated by MyD88 expression and prevention of aberrant TLR/IL1R activation. When PTEN was deleted in phagocytes, a high mortality rate was observed during sepsis, similar to mice treated with a PTEN inhibitor or siPTEN. This indicates that PTEN in myeloid cells mediates the protective effects during sepsis.

In other studies, we demonstrated that genetic and pharmacological PTEN-inhibition improved the phagocytosis of *Candida albicans* (21) and increased bacterial killing of alveolar macrophages infected with IgG-opsonized *Klebsiella pneumonia* (42). PTEN has also been shown to inhibit immune responsiveness to gram-negative lung infections *in vitro* and *in vivo* (17, 18). As it is known that neutrophil migration during infection is essential for the control of sepsis (43), we speculate that increased bacterial counts in PTEN-deficient mice was due to defects in neutrophil migration. Indeed, in previous studies, PTEN deficiency led to impaired neutrophil migration (44) and severe sepsis decreased neutrophil migration to the site of infection dependent on CXCR2 down-regulation (43, 45, 46). However, PTEN's influence on CXCR2 regulates neutrophil migration to the focus of infection remains to be determined. Since PTEN inhibition decreases neutrophil recruitment to the site of infection, these data lead us to hypothesize that macrophages are the key cells involved in the protective effect of PTEN during sepsis. To discriminate between PTEN effects on inflammation and bacterial growth, we co-treated mice with both the PTEN inhibitor Bpvic (OH) and an antibiotic (ertapenem). Interestingly, treating mice with the antibiotic did not rescue the deleterious effect of the PTEN inhibitor in regards to animal lethality. These data indicate that PTEN deficiency leads to an overwhelming inflammatory response, organ damage, and death in response to systemic infection (Fig. S1).

This study identified MyD88 as a major target for PTEN by using a variety of *in vitro* and *in vivo* techniques. PTEN exerts both positive and negative actions during MyD88-dependent TLR/IL1R activation. Genetic and pharmacological PTEN inhibition leads to enhanced LPS

Author Manuscript Author Manuscript Author Manuscript Author Manuscript

responsiveness in macrophages (47). Further, PTEN deficiency increases TLR and IL-1R responsiveness in B cells, lung fibroblasts, and epithelial cells (48, 49). Recently, Aksoy et al. demonstrated that PTEN+/− macrophages exhibited decreased TLR4 membrane translocation during LPS stimulation (50). Here, we observed that MyD88-dependent NF-κB p65 phosphorylation and nitrite production increased in macrophages following PTEN knockdown with siRNA. Although our in blot activity assay showed that PTEN did not dephosphorylate IRAK-4 and IKK alpha, the possibility that PTEN influences other downstream inflammatory effectors or directly influences downstream kinases involved in NF-κB activation cannot be ruled out.

We also further investigated if PTEN was able to control TRIF-dependent macrophage activation. PTEN deficiency did not influence either Poly(I:C)-induced IFN-β production or macrophage IRF-3 phosphorylation. However, Li et al. showed that PTEN increased IFN-α/β−induced IRF3 nuclear translocation and improved antiviral responses in mouse embryonic fibroblasts (51). The difference between our data and this study's results could be due to the stimuli used, Poly(I:C) versus Senday virus or IFN α/β, or the cell lines tested, peritoneal macrophages versus HEK239 cells.

MyD88 expression is controlled via transcriptional and posttranscriptional events (6, 10). PTEN did not affect the expression or phosphorylation of STAT1, a transcription factor responsible for MyD88 expression (6). Furthermore, pharmacologic approaches ruled out a possible participation of the transcription factors STAT1, STAT3 and NFκB in PTEN-mediated MyD88 inhibition. However, we found that PTEN inhibited MyD88 expression by directly controlling the expression of microRNAs that target MyD88. PTEN deletion decreased expression of many microRNAs, including miR125b and miR203, which inhibit MyD88 expression (7, 10). PTEN was also required for optimal microRNA expression in both homeostatic conditions and uncontrolled inflammation, such as sepsis. These data led us to study the role of PTEN in microRNA generation. Surprisingly, PTEN deficiency enhanced the expression of a few microRNAs, including microRNAs involved in inflammatory responses, such as miR155 and let7g. The mechanisms involved remains to be determined, but PTEN may inhibit transcription factors that are involved in microRNA expression, including AP-1 and PU.1 (10, 52).

PTEN also mediated microRNA processing by directly associating with and facilitating translocation of Drosha and Dgcr8 into the nucleus. PTEN is known to shuttle between cellular compartments including the cytoplasm, mitochondria, plasma membrane, endoplasmic reticulum, and nucleus (53). PTEN is found in the nucleus in many normal and cancerous cells and tissues, and some of the molecular mechanisms of PTEN nuclear localization have been described (53). Although PTEN does not have a defined nuclear localization sequence (NLS), it has been proposed that either simple diffusion, a putative cytoplasmic localization signal, active shuttling by the RAN GTPase or major vault protein (MVP), phosphorylation-dependent shuttling, or monoubiquitylation- and sumoylation-dependent nuclear import are responsible for PTEN's cellular location (53). Altered PTEN nucleus/cytoplasm distribution has been linked with various diseases, including cancer and brain-injury and the mechanisms by which PTEN is localized in the nucleus in macrophages are under investigation.

Author Manuscript Author Manuscript Author Manuscript Author Manuscript

The role of PTEN phosphatase activity is controversial, and protein–protein interactions have been suggested to play a major role (53). PTEN SUMOylation sites (K254R and K289R) are responsible for membrane association and nuclear translocation, and this modification is also essential for the inhibition of the PI3K–AKT signaling pathway (39), a finding that correlates with our results that both lipid phosphatase activity and SUMOylation drives microRNA processing. Recently, it has also been shown that SUMOylation is required for optimal microRNA processing and efficacy by influencing both Dicer (54) and the Argonaute-2/RICS complex activity (55, 56). Interestingly, SUMOylation increased Dgcr8 protein stability and promoted its association with pri-miRNAs (57, 58). However, SUMOylation does not influence DROSHA/Dgcr8 association (57). Whether sumoylation influences Drosha activity is unknown. Although PTEN SUMOylation positively controlled PTEN phosphatase activity and nuclear translocation, it remains to be determined if SUMOylation is required for macrophage microRNA expression and processing in vivo. Furthermore, whether changes in PTEN SUMOylation also influence inflammatory responses will be studied.

Interestingly, a well-studied PTEN partner, the tumor suppressor p53, also associates with Drosha and facilitates microRNA processing (59). Whether PTEN is part of a complex formed by p53 and Drosha and other proteins involved in microRNA processing remains to be determined.

In the current study, we dissected the PTEN-associated molecular pathways involved in sepsis. Our results identified a novel regulatory pathway that drives microRNA expression. This work has translation potential given the fact that both PTEN and microRNAs are key players in mediating or exacerbating a myriad of diseases, including cancer, asthma, atherosclerosis, and arthritis (60–67). PTEN and microRNAs may work in concert to prevent aberrant inflammatory responses in different disease settings.

Material and Methods

Study design

In vitro and *in vivo* experiments were designed to test the hypothesis that PTEN prevents SIRS development during sepsis by allowing the expression of microRNAs that target MyD88 expression in phagocytes. For all experiments, the minimum sample size was determined to detect a difference between group means of two times the observed SE, with a power of 0.8 and a significance level of 0.05, using a power and sample size calculator (http://www.statisticalsolutions.net/pss_calc.php). The calculated minimum sample sizes ranged from three to five depending on the experiment. The average sample size for mouse studies was five per group. All samples were randomized but not blinded.

Patients and data collection

The institutional review boards of each participating institution, Cincinnati Children's Hospital Medical Center and Yale School of Medicine, approved the study protocol. Children 10 years of age or younger admitted to the pediatric intensive care unit (PICU) who met pediatric-specific criteria for septic shock were eligible for enrollment (68). Age-

Author Manuscript Author Manuscript Author Manuscript Author Manuscript

matched controls were recruited from the ambulatory departments of participating institutions using published inclusion and exclusion criteria (68). Adults (n = 40) age 19 years or older admitted to the medical intensive care unit (ICU) at Yale New Haven Hospital, Yale School of Medicine, who met the criteria for sepsis (69) were enrolled for RNA isolation obtained from whole blood, based on approval by the Human Investigational Committee. Baseline demographics of the adult septic patients, which included 20 survivors and 20 non-survivors, are outlined in table S1.

Mice

Female and male C57BL/6 mice (8-week old, weight 18–23 g) were obtained from Jackson Laboratory (Bar Harbor, ME, USA). $PTEN^{fl/fl}$ and $PTEN^{fl/fl}$_$LysM^{cre}$ mice were bred at Indiana University School of Medicine and Vanderbilt University Medical Center. Mice were maintained according to NIH guidelines for the use of experimental animals with the approval of the Indiana University and Vanderbilt University Medical Center Committee for the Use and Care of Animals.

Transcriptome data

PTEN mRNA expression data were extracted from an existing, microarray-based transcriptome database. Details of the study protocol were previously published (68), and the data are deposited in the Gene Expression Omnibus (Accession # GSE66099). Briefly, the data reflect children with septic shock (n = 180) and normal controls (n = 52). The RNA used for microarray analyses was derived from whole blood obtained within the first 24 hours of meeting criteria for septic shock. The original consent form for this protocol allows for secondary analysis of clinical and biological data.

The existing, normalized transcriptome data were analyzed using GeneSpring GX 7.3 software (Agilent Technologies, Palo Alto, CA). All signal intensity-based data were used after RMA normalization, which specifically suppresses all but significant variation among lower intensity probe sets (70). All chips representing septic shock samples were then normalized to the respective median values of controls on a per gene basis. Differences in mRNA abundance between study groups were determined using ANOVA and corrections for multiple comparisons using a Benjamini-Hochberg false discovery rate (FDR) of 5%.

Polymicrobial sepsis

Sepsis was induced by CLP, as previously described (71), using a 26-gauge needle to induce moderate sepsis. Survival was monitored at 12 hr intervals for 7 days after CLP surgery. Mice showing signs of imminent death (inability to maintain upright position/ataxia/tremor and or or agonal breathing) were euthanized. For other protocols, mice were euthanized 6 or 24 hr after CLP surgery.

In vitro and *In vivo* pharmacological and genetic treatments

For *in vivo* experiments, mice were treated for 1 hour with 1.5 mg/kg PTEN inhibitor Bpvic(OH) or vehicle control prior to CLP. Sense and antisense strands of murine PTEN siRNA [5′-AGAGAUCGUUAGCAGAAACTT-3′ (sense) and 5′-GUUUCUGCUAACGAUCUCUTT-3′ (antisense)] and scramble (control) siRNA [5′-

Author Manuscript Author Manuscript Author Manuscript Author Manuscript

GCGCGCUUUGUAGGAUUCGTT-3′ (sense) and 5′-CGAAUCCUACAAAGCG CGCTT-3′ (antisense)] were used as previously described (72). All siRNA were synthesized as 2′-deprotected, duplexed, desalted, and purified siRNA form (IdT). To avoid immune stimulation by synthetic siRNA, we incorporated 2'-*O*-methyl (2'OMe) uridine or guanosine nucleosides into one strand of the siRNA duplex. siRNAs were conjugated with in vivo-jetPEI-polyplus transfecting agent with 5% glucose. C57BL/6 mice were treated 48 h prior to moderate CLP. In some experiments, mice were treated with the siRNAs and then treated with 100 μg/Kg MyD88 blocking peptide (DRQIKIWFQNRRMKWKKRDVLPGT) or the scrambled control (DRQIKIWFQNRRMKWKK) with a palmitoyl modification in the N terminus 1 h after CLP. Furthermore, WT mice were pretreated with the PTEN inhibitor as above, followed by CLP. Septic mice were then treated or nor w with the antibiotic ertapenem sodium (30 mg/Kg) s.c. 1 hour after CLP and then every 12 hours thereafter.

For *in vitro* experiments, macrophages were treated with the JAK2 inhibitor AG 490 (1 μM), the STAT3 inhibitor peptide STATTIC V (20 μM), or the NF-κB p65 peptide inhibitor (NF-κB DRQIKIWFQNRRMKWKKQLRRPSDRELSE) or scrambled control (DRQIKIWFQNRRMKWKK) (100 μM each), and Bpvic(OH) (10 nM), PTEN siRNA, or scrambled control siRNA (30 nM each), as we have previously described (21). Macrophages (1×10^6) were incubated with 100 ng/ml LPS, 2 μg/ml PAM3CSK4, or 50 μg/ml Poly(I:C) for 1 h before immunoblotting or 24 h before qPCR assays.

Cell harvest

Elicited macrophages were harvested from the peritoneal cavities of mice by lavage with phosphate-buffered saline (PBS) 4 days after injection of 2 ml 3% thioglycollate, as described previously (6).

Bacterial load and cell counts

Blood was collected from the orbital plexus of mice and the peritoneal cavity was washed with PBS. Aliquots of serial log dilutions were plated in Mueller-Hinton agar dishes, as previously described (71). Leukocyte numbers were determined in the peritoneal cavity and bronchoalveolar lavage fluid (BALF) 6 h after CLP or sham-treatment using the Hemavet 950FS System (71).

Flow cytometry

Peritoneal cells were resuspended in PBS containing 2 mM EDTA and 0.5% FBS. Fc receptor-mediated and nonspecific-antibody binding was blocked with CD16/CD32 (clone 2.4G2, BD Biosciences Pharmingen) for 10 min at 4°C. The cells were stained with mouse anti-GR1-FITC (1:100, BD Pharmingen) for 30 min at 4°C, and expression was analyzed by flow cytometry (FACSCalibur). Data were analyzed with WinMDi and FlowJo Version 7.6.4 software.

Cytokines measurement

TNFα, IL-1β, and IL-6 were measured using DuoSet ELISA (R&D Systems, Minneapolis, MN, USA), following the manufacturer's protocol.

Author Manuscript Author Manuscript Author Manuscript Author Manuscript

Histology

Mice were perfused with 10% formalin before lung harvesting. Tissues were fixed in 10% formalin, embedded in paraffin, cut into 5 μm sections, and stained with H&E, as previously described (71). Images were captured using an Infinity 1 camera attached to Nikon Eclipse Ci microscope. Capillary congestion and alveolar edema were determined as previously described (71).

Immunoblotting

Western blots were performed as previously described (6). Protein samples were resolved by SDS–polyacrylamide gel electrophoresis (SDS-PAGE), transferred to a nitrocellulose membrane, and probed with primary antibodies against MyD88, total or phosphorylated (S727 or Y701) STAT1, phosphorylated p65 NF-κB (Ser 523), PTEN (all at 1:1000; Cell Signaling), TIRAP, TRIF, TIRP, TLR4 (1:1000; Santa Cruz), or β-actin (1:10,000; Sigma-Aldrich). Densitometry analysis was performed as described previously (6).

RNA isolation and semiquantitative real-time RT-PCR

Total RNA from cultured cells was isolated using the GenElute Mammalian Total RNA Miniprep Kit (Sigma) according to the manufacturer's instructions. Real-time RT-PCR (qRT-PCR) was performed as previously described (6). The primers for PTEN, MyD88, primary microRNAs, STAT1, and actin are all from Integrated DNA Technologies. Relative expression was calculated using the comparative threshold cycle (Ct) and expressed relative to control or WT (ΔΔCt method).

Confocal microscopy and PLA

A total of 2×10^5 macrophages from $PTEN^{fl/fl}$ or $PTEN^{fl/fl}$_$LysM^{cre}$ mice were plated in 4-well chamber slides (Nunc) and then washed with PBS. Slide staining was performed as previously described (73) using various combinations of primary antibodies against Drosha, Dgcr8, Dicer, or PTEN (each used at 1:200). Rhodamine- or fluorescein isothiocyanate–conjugated goat anti-rabbit or anti-mouse secondary antibodies (1:200) (Sigma-Aldrich) were used. Cells were imaged on a Zeiss LSM 510 confocal microscope with an inverted Axiovert 100 M microscope stand using a C-apochromat 40×/1.2 W corr. Confocal images were taken with identical settings to allow comparison of staining. Z-stacked sections (10–22 slices) of the cells were captured in multitrack, and image J was used to reconstruct the images using the Z project plug-in. The extent of colocalization between the microRNA machinery and PTEN as well as their intracellular localization was quantitated using the Jacop plug-in for Image J (74). The background of the collected images was corrected by the Image J rolling ball algorithm plug-in. The specific algorithm used was based on the Manders overlap coefficient (74), which ranges from 0 to 1, the former corresponding to non-overlapping images and the latter reflecting 100% colocalization between both images. For each experiment, at least 100 randomly selected cells were scored.

PLA, which allows visualization, localization, and quantification of individual protein interactions at a range of 30 to 40 nm (75), was performed according to the manufacturer's guidelines (Duolink orange detection system; Olink Bioscience, Uppsala, Sweden). Briefly, cells were fixed with 4% paraformaldehyde at room temperature for 10 min, followed by

Author Manuscript Author Manuscript Author Manuscript Author Manuscript

cell-membrane permeabilization with 0.2% Triton X-100 in TBS for 10 min. The cells were then blocked with 1% bovine serum albumin (BSA) plus 10% normal donkey serum in TBS for 1 h at room temperature, and incubated with the indicated primary antibody pairs (Drosha vs. PTEN, Dgcr8 vs. PTEN, and Dicer vs. PTEN) overnight at 4°C. Oligonucleotide-conjugated secondary antibodies (PLA probe MINUS and PLA probe PLUS) against each of the primary antibodies were applied, and ligation as well as amplification was carried out to produce rolling circle products. These products were detected with fluorescent-labeled oligonucleotides and the samples were counterstained using Duolink Mounting Medium with DAPI.

Nuclear isolation

Nuclear and cytoplasmic fractions of peritoneal cells from $PTEN^{fl/fl}$ and $PTEN^{fl/fl}$_lysMcre mice were isolated as previously described (76) (using a subcellular protein fractionation kit, according to the manufacturer's instructions (Pierce).

In-blot PTEN activity assay

PTEN dephosphorylation of IRAK-4 and IKKalpha was examined by an in-blot phosphatase assay as described (21, 77). Briefly, histidine-tagged PTEN (His_6-PTEN) was generated by inserting full-length PTEN complementary DNA (cDNA) into the pQE30 vector (Qiagen). The protein was purified with Ni-NTA beads (Qiagen) under denaturing conditions and then renatured by sequential dilution and concentration in renaturation buffer [PBS (pH 7.0) containing 2 mM $MgCl_2$, 0.5 mM phenylmethanesulfonyl fluoride, 0.005% Tween 20, 10 mM dithiothreitol (DTT), and protease inhibitor mixture]. Purity (>90%) was confirmed by SDS-PAGE and Coomassie blue staining. Peritoneal macrophages (3×10^6) were plated overnight and cells were stimulated with LPS for 1 h, then lysed with radioimmunoprecipitation assay (RIPA) buffer for Western blot. Equal amounts of proteins were subjected to 10% SDS-PAGE and electrotransferred to nitrocellulose. Blots were incubated with recombinant His_6-PTEN (20 μg/ml) or alkaline phosphatase (500 U/ml) in 50 mm Hepes buffer (pH 7.0) containing 10 mm $MgCl_2$ and 10 mm DTT at 30°C for 1 hour. Phosphorylated IRAK-4 and IKK alpha were detected by immunoblot as mentioned above.

Immunoprecipitation

For PTEN immunoprecipitation, macrophages were lysed with RIPA buffer, precleared with protein A–Sepharose for 30 min, and incubated overnight at 4°C with anti-PTEN (1:80) as we have previously shown (21). Protein A–Sepharose was added and incubated for 3 hr with rotation at 4°C. Immunoprecipitates were isolated and subjected to electrophoresis as described above. Membranes were probed with antibodies against PTEN, Drosha, Dgcr8, and Dicer, as described above.

Adenoviral constructs and infection

Adenovirus-containing cDNA constructs encoding constitutively active wild-type PTEN, dominant-negative PTEN (C124S), the lipid phosphatase activity mutant PTEN (G129E), and the empty viral vector (control) containing no cDNA insert were prepared as previously described (21). Adenoviruses were amplified in human embryonic kidney (HEK) 293 cells

Author Manuscript Author Manuscript Author Manuscript Author Manuscript

and purified by ultracentrifugation on a CsCl density gradient. Alveolar or peritoneal macrophages (2×10^6) were seeded in six-well plates in Dulbecco's modified Eagle's medium containing 10% FBS. Virus was added to the medium at an MOI of 250. After 72 h, the cells were harvested and cell lysates were subjected to immunoblotting.

Retrovirus transduction and generation of PTEN mutant MEFS

The $PTEN^{-/-}$ MEFS were grown in DMEM with 10% FBS and penicillin-streptomycin. These cells were reconstituted with wild-type PTEN or mutants of PTEN (C124S, G129E, K254R, and K289R). Briefly, PTEN and mutant PTEN cDNAs were cloned into the pRev-TRE-hygromycin retrovirus construct (Clontech). Retroviral constructs were transfected into 293 Phoenix cells using Lipofectamine. Medium was collected and replaced 24 h after transfection. Medium was collected again after three days. The pooled virus-containing medium was centrifuged, 10 μg/ml of polybrene was added, and the medium was filtered. The filtered virus was added to $PTEN^{-/-}$ MEF cells and incubated for 36 h. The cells were then treated with hygromycin (100 mg/ml) for one week. The surviving cells were maintained in hygromycin (20 mg/ml) and expanded. The hygromycin-resistant cells were analyzed for the presence or absence of PTEN by western blot analysis.

Targeted microRNA overexpression

For inhibition of miR155, 125b, 146b, and 203, macrophages were transfected using Lipofectamine siRNA max transfection reagent with PTEN siRNA or scrambled siRNA control as above, followed by transfection with pre-miR155, 125b, 146b, or pre-miR-negative control 1 (pre-miR control), as we have previously shown (10). Transfected cells were treated with or without 30 nM microRNA mimic for 48 h and, where indicated, treated for 24 h with LPS (100 ng/ml) before collecting supernatants or preparing cell lysates for isolation of RNA (RNeasy kit, Qiagen).

microRNA analysis

qRT-PCR analyses for miR125b, miR125a, miR146a, miR155, miR146b, miR451, miR19a, miR19b, miR203, miR30e, miR21, miR146b, miR181a, let7g, and RNU6 (used as normalization control) were performed using TaqMan microRNA assays with reagents, primers, and probes obtained from Qiagen. cDNA was synthesized using a reverse transcription system (miScript II, Qiagen). qPCR was performed on the CFX96 Real-Time PCR Detection System (Bio-Rad Laboratories) as described (6).

Focused microRNA arrays

To determine the expression of inflammatory microRNAs, macrophages from C57BL/6 WT mice were treated with PTEN siRNA or scrambled siRNA as above. RNA was then extracted from the cells using Qiagen RNeasy mini kit according to the manufacturer's instructions. cDNA was synthesized using the RT2 microRNA First Strand Kit (Qiagen) and applied to PCR focused immunopathology microRNA array plates (Qiagen) as previously shown (10). Normalization and statistical analysis of miRNA expression was conducted using SABiosciences' Online PCR Array Data Analysis Web Portal as previously described (10).

Author Manuscript Author Manuscript Author Manuscript Author Manuscript

AGO2 immunoprecipitation

Macrophages were incubated with 30 nM of microRNA mimic control, miR125b and miR203 for 24 h and a AGO2 was immunoprecipitated using a miRNA target IP kit, according to the manufacturer's instructions (Active Motif). IP with anti-IgG antibody was used as a negative control. After the pull-down; co-precipitated mRNAs were subjected to cDNA and qRT-PCR using primers directed against MyD88 3'UTR and beta2 globulin 3'UTR (IDT Technologies).

Statistical analyses

Survival curves were expressed as percent survival and were analyzed by a Log-rank (Mantel-Cox) Test. Bacterial load results are expressed as median values. Other results are expressed as mean ± SEM and were analyzed by ANOVA followed by Bonferroni analysis. For the pediatric patient group, we performed Mann-Whitney U Statistical analysis. For the adult septic patients, PTEN mRNA expression values were compared by the unpaired Student's t test. In all instances, differences were considered significant when $p<0.05$.

Supplementary Material

Refer to Web version on PubMed Central for supplementary material.

Acknowledgments:

We thank Dr. Daniel Mucida for suggestions.

Funding:

This work was supported by National Institutes of Health Grants [NIH HL-103777; R01HL124159-01 (CHS); T32AI060519 (SB); GM099773 and GM108025 (HW)], American Lung Association Senior Research Training Fellowship (RT-349159 (NB), CAPES and São Paulo Research Foundation (FAPESP) under grant agreements n° 2011/19670-0 (Projeto Temático) and 2013/08216-2 (Center for Research in Inflammatory Disease).

References and Notes

1. Hotchkiss RS, Karl IE, The pathophysiology and treatment of sepsis. The New England journal of medicine 348, 138–150 (2003). [PubMed: 12519925]
2. Okin D, Medzhitov R, Evolution of inflammatory diseases. Current biology : CB 22, R733–740 (2012). [PubMed: 22975004]
3. Warner N, Nunez G, MyD88: a critical adaptor protein in innate immunity signal transduction. J Immunol 190, 3–4 (2013). [PubMed: 23264668]
4. Netea MG, Wijmenga C, O'Neill LA, Genetic variation in Toll-like receptors and disease susceptibility. Nature immunology 13, 535–542 (2012). [PubMed: 22610250]
5. Zarember KA, Godowski PJ, Tissue expression of human Toll-like receptors and differential regulation of Toll-like receptor mRNAs in leukocytes in response to microbes, their products, and cytokines. J Immunol 168, 554–561 (2002). [PubMed: 11777946]
6. Serezani CH, Lewis C, Jancar S, Peters-Golden M, Leukotriene B4 amplifies NF-kappaB activation in mouse macrophages by reducing SOCS1 inhibition of MyD88 expression. The Journal of clinical investigation 121, 671–682 (2011). [PubMed: 21206089]
7. Wei J, Huang X, Zhang Z, Jia W, Zhao Z, Zhang Y, Liu X, Xu G, MyD88 as a target of microRNA-203 in regulation of lipopolysaccharide or Bacille Calmette-Guerin induced inflammatory response of macrophage RAW264.7 cells. Molecular immunology 55, 303–309 (2013). [PubMed: 23522925]

Author Manuscript Author Manuscript Author Manuscript Author Manuscript

8. Wendlandt EB, Graff JW, Gioannini TL, McCaffrey AP, Wilson ME, The role of microRNAs miR-200b and miR-200c in TLR4 signaling and NF-kappaB activation. Innate immunity 18, 846–855 (2012). [PubMed: 22522429]
9. He L, Hannon GJ, MicroRNAs: small RNAs with a big role in gene regulation. Nat Rev Genet 5, 522–531 (2004). [PubMed: 15211354]
10. Wang Z, Filgueiras LR, Wang S, Serezani AP, Peters-Golden M, Jancar S, Serezani CH, Leukotriene B4 enhances the generation of proinflammatory microRNAs to promote MyD88-dependent macrophage activation. J Immunol 192, 2349–2356 (2014). [PubMed: 24477912]
11. Squadrito ML, Etzrodt M, De Palma M, Pittet MJ, MicroRNA-mediated control of macrophages and its implications for cancer. Trends in immunology 34, 350–359 (2013). [PubMed: 23498847]
12. Vanhaesebroeck B, Stephens L, Hawkins P, PI3K signalling: the path to discovery and understanding. Nature reviews. Molecular cell biology 13, 195–203 (2012).
13. Daikoku T, Dey SK, Two faces of PTEN. Nature medicine 14, 1192–1193 (2008).
14. Choi YJ, Jung J, Chung HK, Im E, Rhee SH, PTEN regulates TLR5-induced intestinal inflammation by controlling Mal/TIRAP recruitment. FASEB journal : official publication of the Federation of American Societies for Experimental Biology 27, 243–254 (2013). [PubMed: 23038756]
15. Cao X, Wei G, Fang H, Guo J, Weinstein M, Marsh CB, Ostrowski MC, Tridandapani S, The inositol 3-phosphatase PTEN negatively regulates Fc gamma receptor signaling, but supports Toll-like receptor 4 signaling in murine peritoneal macrophages. J Immunol 172, 4851–4857 (2004). [PubMed: 15067063]
16. Lee SH, Lee YP, Kim SY, Jeong MS, Lee MJ, Kang HW, Jeong HJ, Kim DW, Sohn EJ, Jang SH, Kim YH, Kwon HJ, Cho SW, Park J, Eum WS, Choi SY, Inhibition of LPS-induced cyclooxygenase 2 and nitric oxide production by transduced PEP-1-PTEN fusion protein in Raw 264.7 macrophage cells. Experimental & molecular medicine 40, 629–638 (2008). [PubMed: 19116448]
17. Hubbard LL, Wilke CA, White ES, Moore BB, PTEN limits alveolar macrophage function against Pseudomonas aeruginosa after bone marrow transplantation. American journal of respiratory cell and molecular biology 45, 1050–1058 (2011). [PubMed: 21527775]
18. Schabbauer G, Matt U, Gunzl P, Warszawska J, Furtner T, Hainzl E, Elbau I, Mesteri I, Doninger B, Binder BR, Knapp S, Myeloid PTEN promotes inflammation but impairs bactericidal activities during murine pneumococcal pneumonia. J Immunol 185, 468–476 (2010). [PubMed: 20505137]
19. Aksoy E, Taboubi S, Torres D, Delbauve S, Hachani A, Whitehead MA, Pearce WP, Berenjeno-Martin I, Nock G, Filloux A, Beyaert R, Flamand V, Vanhaesebroeck B, The p110delta isoform of the kinase PI(3)K controls the subcellular compartmentalization of TLR4 signaling and protects from endotoxic shock. Nature immunology 14, 877 (2013).
20. Koul D, Yao Y, Abbruzzese JL, Yung WK, Reddy SA, Tumor suppressor MMAC/PTEN inhibits cytokine-induced NFkappaB activation without interfering with the IkappaB degradation pathway. The Journal of biological chemistry 276, 11402–11408 (2001). [PubMed: 11278366]
21. Serezani CH, Kane S, Medeiros AI, Cornett AM, Kim SH, Marques MM, Lee SP, Lewis C, Bourdonnay E, Ballinger MN, White ES, Peters-Golden M, PTEN directly activates the actin depolymerization factor cofilin-1 during PGE2-mediated inhibition of phagocytosis of fungi. Sci Signal 5, ra12 (2012). [PubMed: 22317922]
22. Benjamim CF, Hogaboam CM, Kunkel SL, The chronic consequences of severe sepsis. Journal of leukocyte biology 75, 408–412 (2004). [PubMed: 14557384]
23. Oberholzer A, Oberholzer C, Moldawer LL, Sepsis syndromes: understanding the role of innate and acquired immunity. Shock 16, 83–96 (2001). [PubMed: 11508871]
24. Castaldo ET, Yang EY, Severe sepsis attributable to community-associated methicillin-resistant Staphylococcus aureus: an emerging fatal problem. The American surgeon 73, 684–687; discussion 687–688 (2007). [PubMed: 17674941]
25. Bosmann M, Ward PA, The inflammatory response in sepsis. Trends in immunology 34, 129–136 (2013). [PubMed: 23036432]
26. Takeda K, Akira S, Microbial recognition by Toll-like receptors. Journal of dermatological science 34, 73–82 (2004). [PubMed: 15033189]

Author Manuscript Author Manuscript Author Manuscript Author Manuscript

27. O'Neill LA, Golenbock D, Bowie AG, The history of Toll-like receptors - redefining innate immunity. Nature reviews. Immunology 13, 453–460 (2013).
28. O'Neill LA, Bowie AG, The family of five: TIR-domain-containing adaptors in Toll-like receptor signalling. Nature reviews. Immunology 7, 353–364 (2007).
29. Akira S, Takeda K, Toll-like receptor signalling. Nature reviews. Immunology 4, 499–511 (2004).
30. Zhou H, Gao S, Duan X, Liang S, Scott DA, Lamont RJ, Wang H, Inhibition of serum- and glucocorticoid-inducible kinase 1 enhances TLR-mediated inflammation and promotes endotoxin-driven organ failure. FASEB journal : official publication of the Federation of American Societies for Experimental Biology 29, 3737–3749 (2015). [PubMed: 25993992]
31. Schust J, Sperl B, Hollis A, Mayer TU, Berg T, Stattic: a small-molecule inhibitor of STAT3 activation and dimerization. Chem Biol 13, 1235–1242 (2006). [PubMed: 17114005]
32. He X, Jing Z, Cheng G, MicroRNAs: new regulators of Toll-like receptor signalling pathways. Biomed Res Int 2014, 945169 (2014). [PubMed: 24772440]
33. Virtue A, Wang H, Yang XF, MicroRNAs and toll-like receptor/interleukin-1 receptor signaling. Journal of hematology & oncology 5, 66 (2012). [PubMed: 23078795]
34. Quinn EM, Wang J, Redmond HP, The emerging role of microRNA in regulation of endotoxin tolerance. Journal of leukocyte biology 91, 721–727 (2012). [PubMed: 22389313]
35. O'Neill LA, Sheedy FJ, McCoy CE, MicroRNAs: the fine-tuners of Toll-like receptor signalling. Nature reviews. Immunology 11, 163–175 (2011).
36. Nahid MA, Satoh M, Chan EK, MicroRNA in TLR signaling and endotoxin tolerance. Cellular & molecular immunology 8, 388–403 (2011). [PubMed: 21822296]
37. Iwakawa HO, Tomari Y, The Functions of MicroRNAs: mRNA Decay and Translational Repression. Trends in cell biology 25, 651–665 (2015). [PubMed: 26437588]
38. Meng Z, Jia LF, Gan YH, PTEN activation through K163 acetylation by inhibiting HDAC6 contributes to tumour inhibition. Oncogene, (2015).
39. Huang J, Yan J, Zhang J, Zhu S, Wang Y, Shi T, Zhu C, Chen C, Liu X, Cheng J, Mustelin T, Feng GS, Chen G, Yu J, SUMO1 modification of PTEN regulates tumorigenesis by controlling its association with the plasma membrane. Nature communications 3, 911 (2012).
40. Trotman LC, Wang X, Alimonti A, Chen Z, Teruya-Feldstein J, Yang H, Pavletich NP, Carver BS, Cordon-Cardo C, Erdjument-Bromage H, Tempst P, Chi SG, Kim HJ, Misteli T, Jiang X, Pandolfi PP, Ubiquitination regulates PTEN nuclear import and tumor suppression. Cell 128, 141–156 (2007). [PubMed: 17218261]
41. Bi Y, Liu G, Yang R, MicroRNAs: novel regulators during the immune response. Journal of cellular physiology 218, 467–472 (2009). [PubMed: 19034913]
42. Canetti C, Serezani CH, Atrasz RG, White ES, Aronoff DM, Peters-Golden M, Activation of phosphatase and tensin homolog on chromosome 10 mediates the inhibition of FcgammaR phagocytosis by prostaglandin E2 in alveolar macrophages. J Immunol 179, 8350–8356 (2007). [PubMed: 18056380]
43. Alves-Filho JC, de Freitas A, Spiller F, Souto FO, Cunha FQ, The role of neutrophils in severe sepsis. Shock 30 Suppl 1, 3–9 (2008).
44. Heit B, Robbins SM, Downey CM, Guan Z, Colarusso P, Miller BJ, Jirik FR, Kubes P, PTEN functions to 'prioritize' chemotactic cues and prevent 'distraction' in migrating neutrophils. Nature immunology 9, 743–752 (2008). [PubMed: 18536720]
45. Alves-Filho JC, Freitas A, Souto FO, Spiller F, Paula-Neto H, Silva JS, Gazzinelli RT, Teixeira MM, Ferreira SH, Cunha FQ, Regulation of chemokine receptor by Toll-like receptor 2 is critical to neutrophil migration and resistance to polymicrobial sepsis. Proceedings of the National Academy of Sciences of the United States of America 106, 4018–4023 (2009). [PubMed: 19234125]
46. Rios-Santos F, Alves-Filho JC, Souto FO, Spiller F, Freitas A, Lotufo CM, Soares MB, Dos Santos RR, Teixeira MM, Cunha FQ, Down-regulation of CXCR2 on neutrophils in severe sepsis is mediated by inducible nitric oxide synthase-derived nitric oxide. American journal of respiratory and critical care medicine 175, 490–497 (2007). [PubMed: 17138957]
47. Tachado SD, Li X, Swan K, Patel N, Koziel H, Constitutive activation of phosphatidylinositol 3-kinase signaling pathway down-regulates TLR4-mediated tumor necrosis factor-alpha release in

Author Manuscript Author Manuscript Author Manuscript Author Manuscript

alveolar macrophages from asymptomatic HIV-positive persons in vitro. The Journal of biological chemistry 283, 33191–33198 (2008). [PubMed: 18826950]

48. He Z, Deng Y, Li W, Chen Y, Xing S, Zhao X, Ding J, Gao Y, Wang X, Overexpression of PTEN suppresses lipopolysaccharide-induced lung fibroblast proliferation, differentiation and collagen secretion through inhibition of the PI3-K-Akt-GSK3beta pathway. Cell Biosci 4, 2 (2014). [PubMed: 24387036]
49. Zhong LM, Zong Y, Sun L, Guo JZ, Zhang W, He Y, Song R, Wang WM, Xiao CJ, Lu D, Resveratrol inhibits inflammatory responses via the mammalian target of rapamycin signaling pathway in cultured LPS-stimulated microglial cells. PloS one 7, e32195 (2012). [PubMed: 22363816]
50. Aksoy E, Taboubi S, Torres D, Delbauve S, Hachani A, Whitehead MA, Pearce WP, Berenjeno IM, Nock G, Filloux A, Beyaert R, Flamand V, Vanhaesebroeck B, The p110delta isoform of the kinase PI(3)K controls the subcellular compartmentalization of TLR4 signaling and protects from endotoxic shock. Nature immunology 13, 1045–1054 (2012). [PubMed: 23023391]
51. Li S, Zhu M, Pan R, Fang T, Cao YY, Chen S, Zhao X, Lei CQ, Guo L, Chen Y, Li CM, Jokitalo E, Yin Y, Shu HB, Guo D, The tumor suppressor PTEN has a critical role in antiviral innate immunity. Nature immunology 17, 241–249 (2016). [PubMed: 26692175]
52. Ghani S, Riemke P, Schonheit J, Lenze D, Stumm J, Hoogenkamp M, Lagendijk A, Heinz S, Bonifer C, Bakkers J, Abdelilah-Seyfried S, Hummel M, Rosenbauer F, Macrophage development from HSCs requires PU.1-coordinated microRNA expression. Blood 118, 2275–2284 (2011). [PubMed: 21730352]
53. Baker SJ, PTEN enters the nuclear age. Cell 128, 25–28 (2007). [PubMed: 17218252]
54. Gross TJ, Powers LS, Boudreau RL, Brink B, Reisetter A, Goel K, Gerke AK, Hassan IH, Monick MM, A microRNA processing defect in smokers' macrophages is linked to SUMOylation of the endonuclease DICER. The Journal of biological chemistry 289, 12823–12834 (2014). [PubMed: 24668803]
55. Josa-Prado F, Henley JM, Wilkinson KA, SUMOylation of Argonaute-2 regulates RNA interference activity. Biochemical and biophysical research communications 464, 1066–1071 (2015). [PubMed: 26188511]
56. Sahin U, Lapaquette P, Andrieux A, Faure G, Dejean A, Sumoylation of human argonaute 2 at lysine-402 regulates its stability. PloS one 9, e102957 (2014). [PubMed: 25036361]
57. Zhu C, Chen C, Huang J, Zhang H, Zhao X, Deng R, Dou J, Jin H, Chen R, Xu M, Chen Q, Wang Y, Yu J, SUMOylation at K707 of DGCR8 controls direct function of primary microRNA. Nucleic acids research 43, 7945–7960 (2015). [PubMed: 26202964]
58. Zhu C, Chen C, Chen R, Deng R, Zhao X, Zhang H, Duo J, Chen Q, Jin H, Wang Y, Huang J, Xu M, Yu J, K259-SUMOylation of DGCR8 promoted by p14ARF exerts a tumor-suppressive function. Journal of molecular cell biology, (2016).
59. He L, He X, Lim LP, de Stanchina E, Xuan Z, Liang Y, Xue W, Zender L, Magnus J, Ridzon D, Jackson AL, Linsley PS, Chen C, Lowe SW, Cleary MA, Hannon GJ, A microRNA component of the p53 tumour suppressor network. Nature 447, 1130–1134 (2007). [PubMed: 17554337]
60. Ke B, Shen XD, Ji H, Kamo N, Gao F, Freitas MC, Busuttil RW, Kupiec-Weglinski JW, HO-1-STAT3 axis in mouse liver ischemia/reperfusion injury: regulation of TLR4 innate responses through PI3K/PTEN signaling. Journal of hepatology 56, 359–366 (2012). [PubMed: 21756853]
61. Koide S, Okazaki M, Tamura M, Ozumi K, Takatsu H, Kamezaki F, Tanimoto A, Tasaki H, Sasaguri Y, Nakashima Y, Otsuji Y, PTEN reduces cuff-induced neointima formation and proinflammatory cytokines. American journal of physiology. Heart and circulatory physiology 292, H2824–2831 (2007). [PubMed: 17277022]
62. Lee KS, Park SJ, Hwang PH, Yi HK, Song CH, Chai OH, Kim JS, Lee MK, Lee YC, PPAR-gamma modulates allergic inflammation through up-regulation of PTEN. FASEB journal : official publication of the Federation of American Societies for Experimental Biology 19, 1033–1035 (2005). [PubMed: 15788448]
63. Chen R, Alvero AB, Silasi DA, Steffensen KD, Mor G, Cancers take their Toll--the function and regulation of Toll-like receptors in cancer cells. Oncogene 27, 225–233 (2008). [PubMed: 18176604]

Author Manuscript Author Manuscript Author Manuscript Author Manuscript

64. Sharma A, Kumar M, Ahmad T, Mabalirajan U, Aich J, Agrawal A, Ghosh B, Antagonism of mmu-mir-106a attenuates asthma features in allergic murine model. J Appl Physiol 113, 459–464 (2012). [PubMed: 22700801]

65. Zhang E, Wu Y, MicroRNAs: important modulators of oxLDL-mediated signaling in atherosclerosis. Journal of atherosclerosis and thrombosis 20, 215–227 (2013). [PubMed: 23064493]

66. Sheedy FJ, O'Neill LA, Adding fuel to fire: microRNAs as a new class of mediators of inflammation. Annals of the rheumatic diseases 67 Suppl 3, iii50–55 (2008). [PubMed: 19022814]

67. Bluml S, Friedrich M, Lohmeyer T, Sahin E, Saferding V, Brunner J, Puchner A, Mandl P, Niederreiter B, Smolen JS, Schabbauer G, Redlich K, Loss of phosphatase and tensin homolog (PTEN) in myeloid cells controls inflammatory bone destruction by regulating the osteoclastogenic potential of myeloid cells. Annals of the rheumatic diseases 74, 227–233 (2015). [PubMed: 24078675]

68. Wong HR, Shanley TP, Sakthivel B, Cvijanovich N, Lin R, Allen GL, Thomas NJ, Doctor A, Kalyanaraman M, Tofil NM, Penfil S, Monaco M, Tagavilla MA, Odoms K, Dunsmore K, Barnes M, Aronow BJ, Genome-level expression profiles in pediatric septic shock indicate a role for altered zinc homeostasis in poor outcome. Physiol Genomics 30, 146–155 (2007). [PubMed: 17374846]

69. Dellinger RP, Levy MM, Rhodes A, Annane D, Gerlach H, Opal SM, Sevransky JE, Sprung CL, Douglas IS, Jaeschke R, Osborn TM, Nunnally ME, Townsend SR, Reinhart K, Kleinpell RM, Angus DC, Deutschman CS, Machado FR, Rubenfeld GD, Webb SA, Beale RJ, Vincent JL, Moreno R, Surviving S Sepsis Campaign Guidelines Committee including the Pediatric, Surviving sepsis campaign: international guidelines for management of severe sepsis and septic shock: 2012. Critical care medicine 41, 580–637 (2013). [PubMed: 23353941]

70. Irizarry RA, Hobbs B, Collin F, Beazer-Barclay YD, Antonellis KJ, Scherf U, Speed TP, Exploration, normalization, and summaries of high density oligonucleotide array probe level data. Biostatistics 4, 249–264 (2003). [PubMed: 12925520]

71. Ferreira AE, Sisti F, Sonego F, Wang S, Filgueiras LR, Brandt S, Serezani AP, Du H, Cunha FQ, Alves-Filho JC, Serezani CH, PPAR-gamma/IL-10 axis inhibits MyD88 expression and ameliorates murine polymicrobial sepsis. J Immunol 192, 2357–2365 (2014). [PubMed: 24489087]

72. Kamo N, Ke B, Busuttil RW, Kupiec-Weglinski JW, PTEN-mediated Akt/beta-catenin/Foxo1 signaling regulates innate immune responses in mouse liver ischemia/reperfusion injury. Hepatology 57, 289–298 (2013). [PubMed: 22807038]

73. Serezani CH, Aronoff DM, Sitrin RG, Peters-Golden M, FcgammaRI ligation leads to a complex with BLT1 in lipid rafts that enhances rat lung macrophage antimicrobial functions. Blood 114, 3316–3324 (2009). [PubMed: 19657115]

74. Bolte S, Cordelieres FP, A guided tour into subcellular colocalization analysis in light microscopy. J Microsc 224, 213–232 (2006). [PubMed: 17210054]

75. Wu YH, Lai MZ, Measuring NLR Oligomerization V: In Situ Proximity Ligation Assay. Methods Mol Biol 1417, 185–195 (2016). [PubMed: 27221490]

76. Filgueiras LR, Brandt SL, Wang S, Wang Z, Morris DL, Evans-Molina C, Mirmira RG, Jancar S, Serezani CH, Leukotriene B4-mediated sterile inflammation promotes susceptibility to sepsis in a mouse model of type 1 diabetes. Science signaling 8, ra10 (2015). [PubMed: 25628460]

77. White ES, Atrasz RG, Hu B, Phan SH, Stambolic V, Mak TW, Hogaboam CM, Flaherty KR, Martinez FJ, Kontos CD, Toews GB, Negative regulation of myofibroblast differentiation by PTEN (Phosphatase and Tensin Homolog Deleted on chromosome 10). American journal of respiratory and critical care medicine 173, 112–121 (2006). [PubMed: 16179636]

Author Manuscript Author Manuscript Author Manuscript Author Manuscript

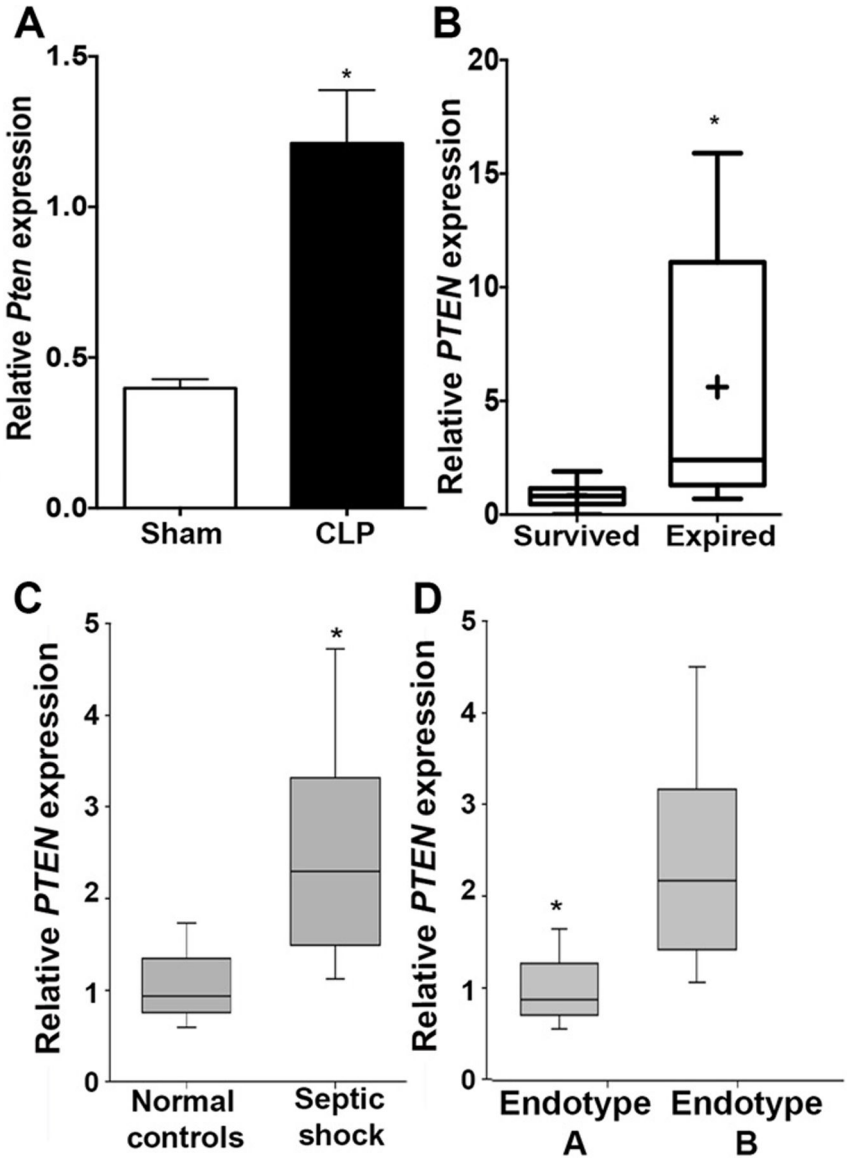

Figure 1. *PTEN* mRNA abundance is increased in murine sepsis and in the blood of septic pediatric and adult patients.

(A) qPCR analysis of *Pten* mRNA expression in murine peritoneal cells 6 h after CLP-induced sepsis or sham-treated controls. $n = 8$ mice/group, t test, Mann-Whitney U test). (B) qPCR analysis of *PTEN* mRNA expression in the blood of adult septic patients that either survived (n = 18) or died (expired, n = 22). (C) *PTEN* mRNA abundance in the blood of normal control subjects (n = 52) and septic pediatric patients (n = 180) as determined by qPCR. (D) *PTEN* mRNA abundance in the blood of pediatric septic patients that either developed co-morbidities (endotype A, n = 60) or not (endotype B, n = 160) as determined by qPCR. Data in B-D were analyzed by ANOVA, and corrections for multiple comparisons were performed using a Benjamini-Hochberg false discovery rate of 5%. Data are expressed as relative abundance to normal control subjects. For all data, *$p<0.05$ compared to sham, surviving patients, normal controls, or endotype B.

Author Manuscript Author Manuscript Author Manuscript Author Manuscript

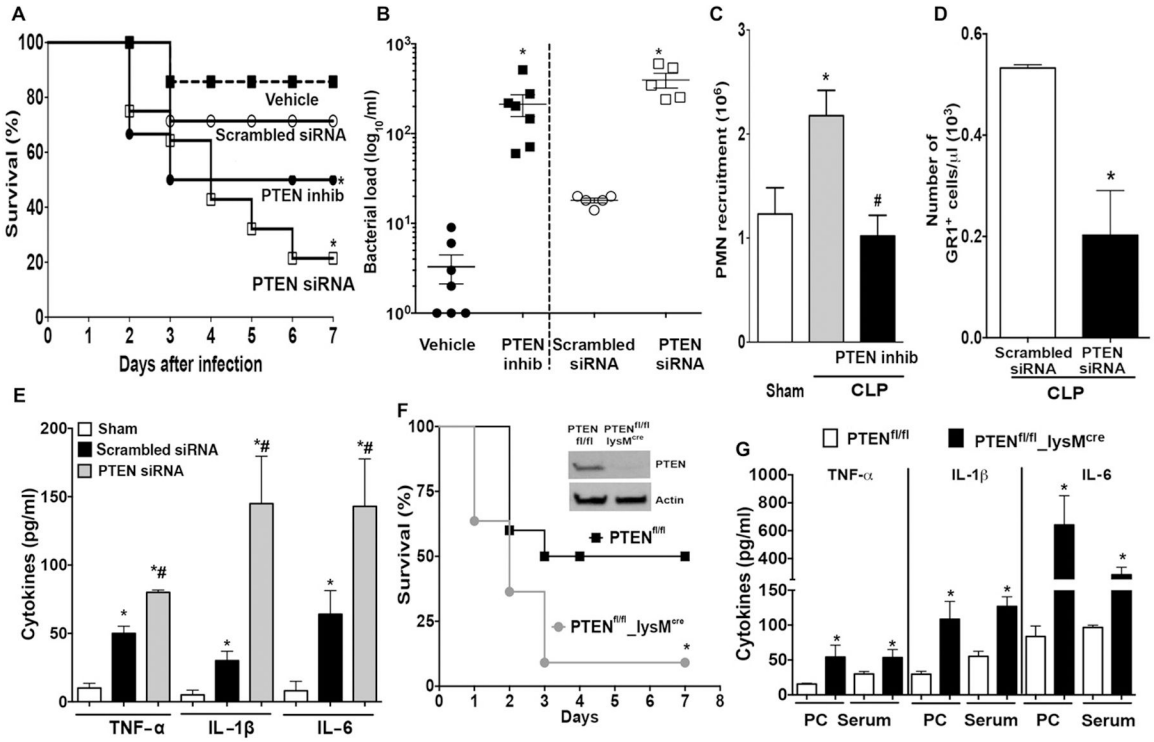

Figure 2. Myeloid PTEN inhibits SIRS and improves animal survival and bacterial clearance during sepsis.

(A) Survival rates of C57BL/6 mice treated with scrambled siRNA control or PTEN siRNA, or treated with vehicle or the PTEN inhibitor Bpvic(OH) prior to receiving moderate CLP. Survival was monitored for 7 days (n = 10 mice/group; log-rank [Mantel-Cox] test). (B, C, D) The peritoneal exudate of mice treated with the indicated inhibitor or siRNA was isolated 6 h after CLP-induced sepsis. Bacterial burden (B) and neutrophil recruitment (C and D) were determined. (n = 7 mice/group, 1-way ANOVA followed by Bonferroni correction). PMN, polymorph nuclear cell (E) Concentrations of IL-1β, TNFα, and IL-6 in the peritoneal exudate of mice treated as in (A) (n = 7 mice/group; 1-way ANOVA followed by Bonferroni correction.). (F) Survival rates of $PTEN^{fl/fl}$ (control) and $PTEN^{fl/fl}$_$lysM^{cre}$ mice subjected to moderate CLP-induced sepsis. Survival was monitored for 7 days (n = 14 mice/group; log-rank [Mantel-Cox] test). Inset shows the abundance of PTEN and actin internal control by Western blot in peritoneal cells from $PTEN^{fl/fl}$ and $PTEN^{fl/fl}$_$lysM^{cre}$ mice. (G) Production of TNFα, IL-1β, and IL-6 in the serum and peritoneal cavity 6 h after CLP-induced sepsis in $PTEN^{fl/fl}$ and $PTEN^{fl/fl}$_$lysM^{cre}$ mice (n = 7 mice/group; 1-way ANOVA followed by Bonferroni correction). For all data, *p<0.05 compared to sham mice, vehicle, scrambled siRNA control, or $PTEN^{fl/fl}$. PTEN inhib, Bpvic(OH); PC, peritoneal cavity

Author Manuscript Author Manuscript Author Manuscript Author Manuscript

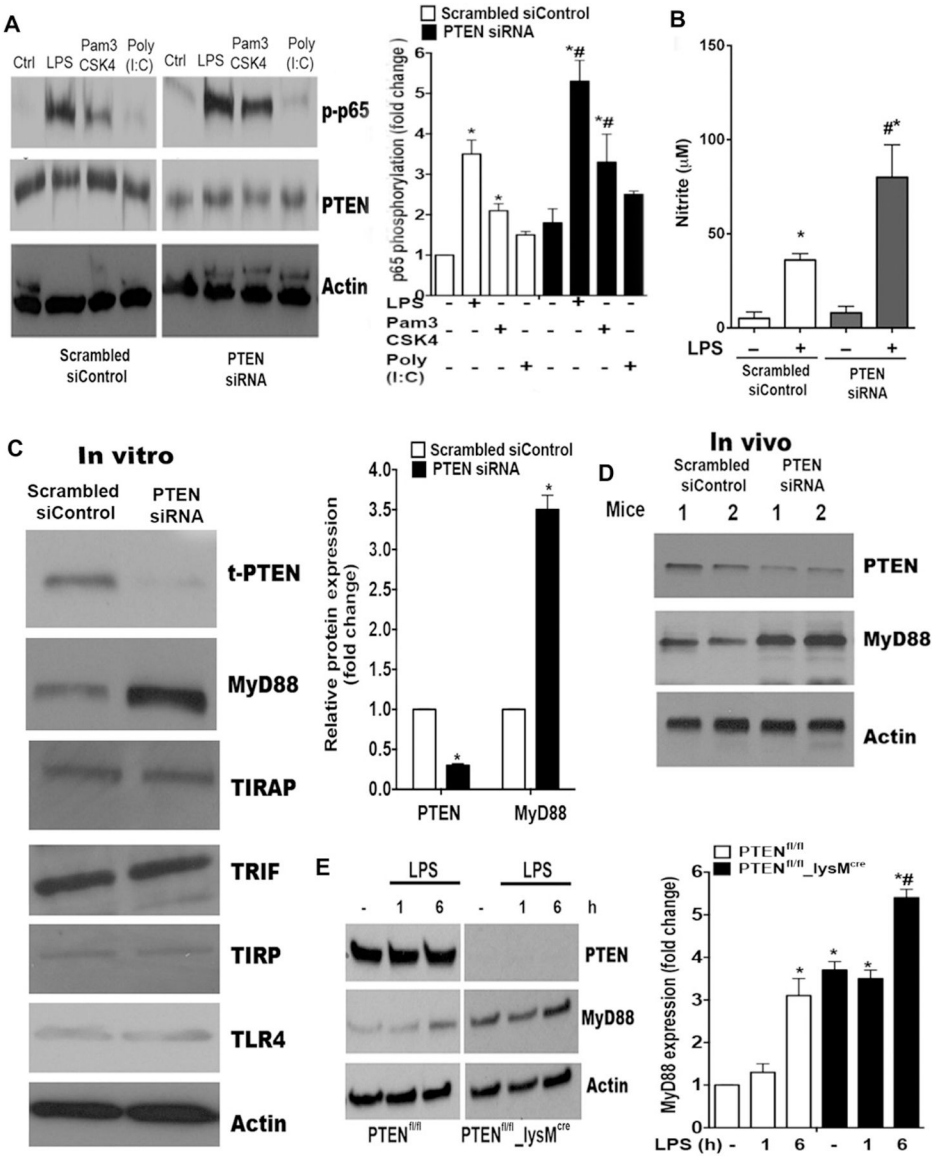

Figure 3. PTEN inhibits MyD88 expression and prevents TLR2 and TLR4 activation in macrophages.

(A) Isolated macrophages were transfected with scrambled or PTEN siRNA for 48 h and stimulated with TLR agonists for 30 min. Left - The phosphorylated form on the NF-κB subunit p65 (p-p65), PTEN, and actin abundance were determined by immunoblot. Right - Quantification of at least 3 independent experiments is shown in the graph as the mean ± SEM. (B) Macrophages transfected as in (A) were left unstimulated or were stimulated with LPS for 24 h and nitrite abundance was determined in the supernatant by Griess assay. Quantification of at least 3 independent experiments is shown in the graph as the mean ± SEM. (C) Right - Macrophages were transfected as in (A) and expression of the indicated proteins was determined by immunoblot. t-PTEN is total PTEN. Left - Quantification of PTEN and MyD88 from at least 3 independent experiments are shown in the graph as the mean ± SEM. (D) Wild-type mice were injected intraperitoneally with scrambled siRNA or PTEN siRNA. PTEN and MyD88 protein abundance were determined in resident peritoneal

Author Manuscript Author Manuscript Author Manuscript Author Manuscript

cells by immunoblot. Data are from two mice/group. (E) Right - Macrophages from $PTEN^{fl/fl}$ and $PTEN^{fl/fl}$_$lysM^{cre}$ mice were challenged with LPS for the indicated time, and MyD88 abundance was determined by immunoblot. Left - Quantification of at least 3 independent experiments is shown in the graph as the mean ± SEM. For all data, $^{*}p<0.05$ compared to scramble siRNA control group or $PTEN^{fl/fl}$; $^{\#}p<0.05$ LPS-stimulated PTEN siRNA or $PTEN^{fl/fl}$_$lysM^{cre}$ compared to scramble siRNA control group or $PTEN^{fl/fl}$ macrophages. In all circumstances, at least 3 independent experiments were performed and 1-way ANOVA followed by Bonferroni correction.

Author Manuscript Author Manuscript Author Manuscript Author Manuscript

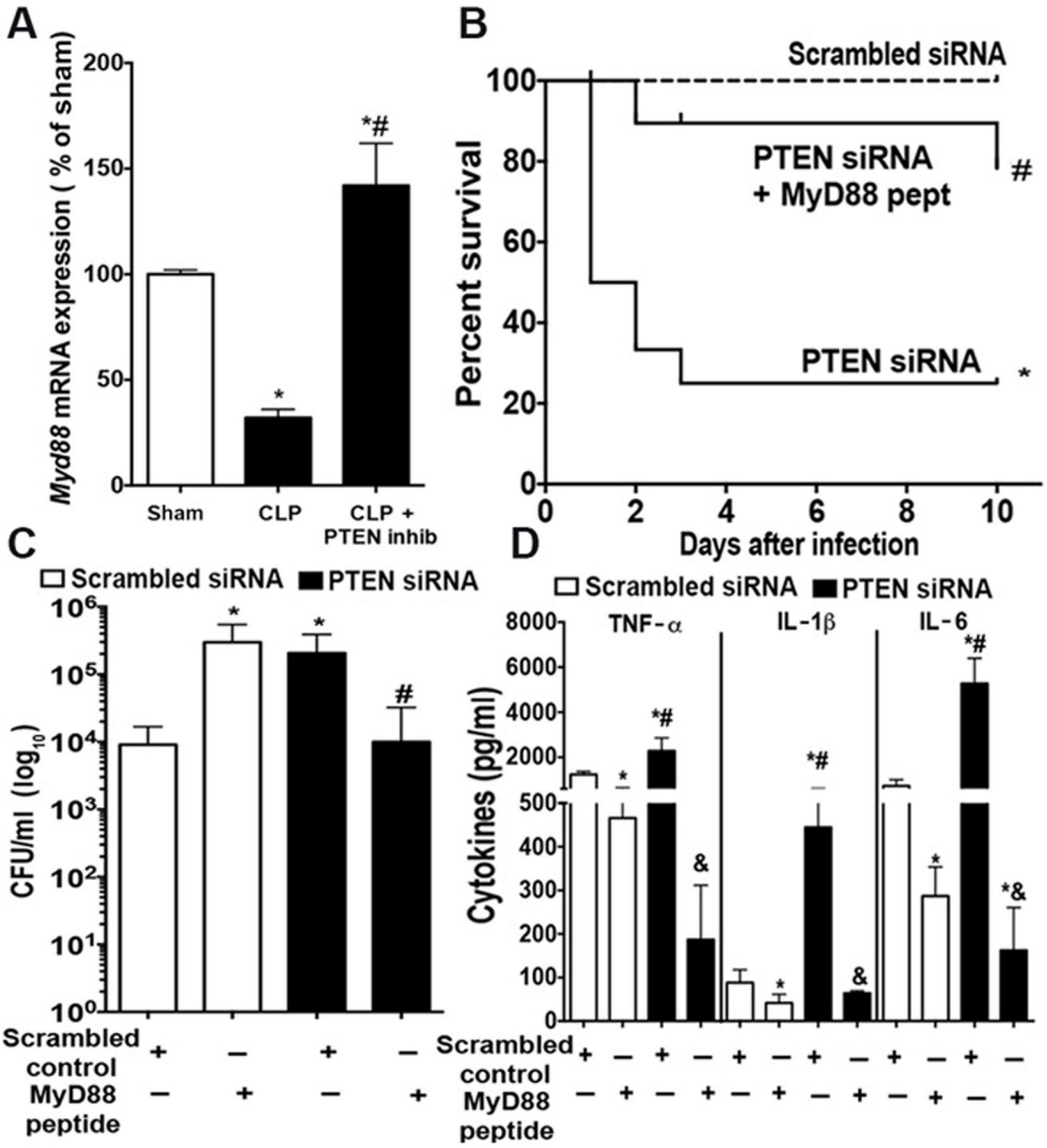

Figure 4. Blocking MyD88 prevents enhanced mortality, bacterial load, and prevents SIRS in siPTEN-challenged mice.

(A) C57BL/6 mice were treated with PTEN inhibitor (inhib) or vehicle control 24 h before CLP-induced sepsis. *Myd88* mRNA abundance was determined in peritoneal cells 24 h after sepsis by qPCR. Abundance relative to Sham-operated mice expressed as mean ± SEM is shown. (n = 4–6 mice/group; 1-way ANOVA followed by Bonferroni correction). (B) Wild-type mice were treated with scrambled siRNA control or PTEN siRNA prior to receiving CLP, followed by MyD88 peptide inhibitor (pept) treatment for 1 h after CLP. Survival was monitored for 7 days (n = 13 mice/group; log-rank [Mantel-Cox] test). (C, D) Wild-type mice were treated as in (B) and bacterial burden (C) and cytokine production (D) were determined in peritoneal exudates 24 h after CLP. Data are expressed as mean ± SEM from at least 5 mice/group; 1-way ANOVA followed by Bonferroni correction. For all data, *$p<0.01$ compared to sham, vehicle control, scramble siRNA control, or $PTEN^{fl/fl}$; $^{\#}p<0.01$ compared to PTEN siRNA group.

Author Manuscript Author Manuscript Author Manuscript Author Manuscript

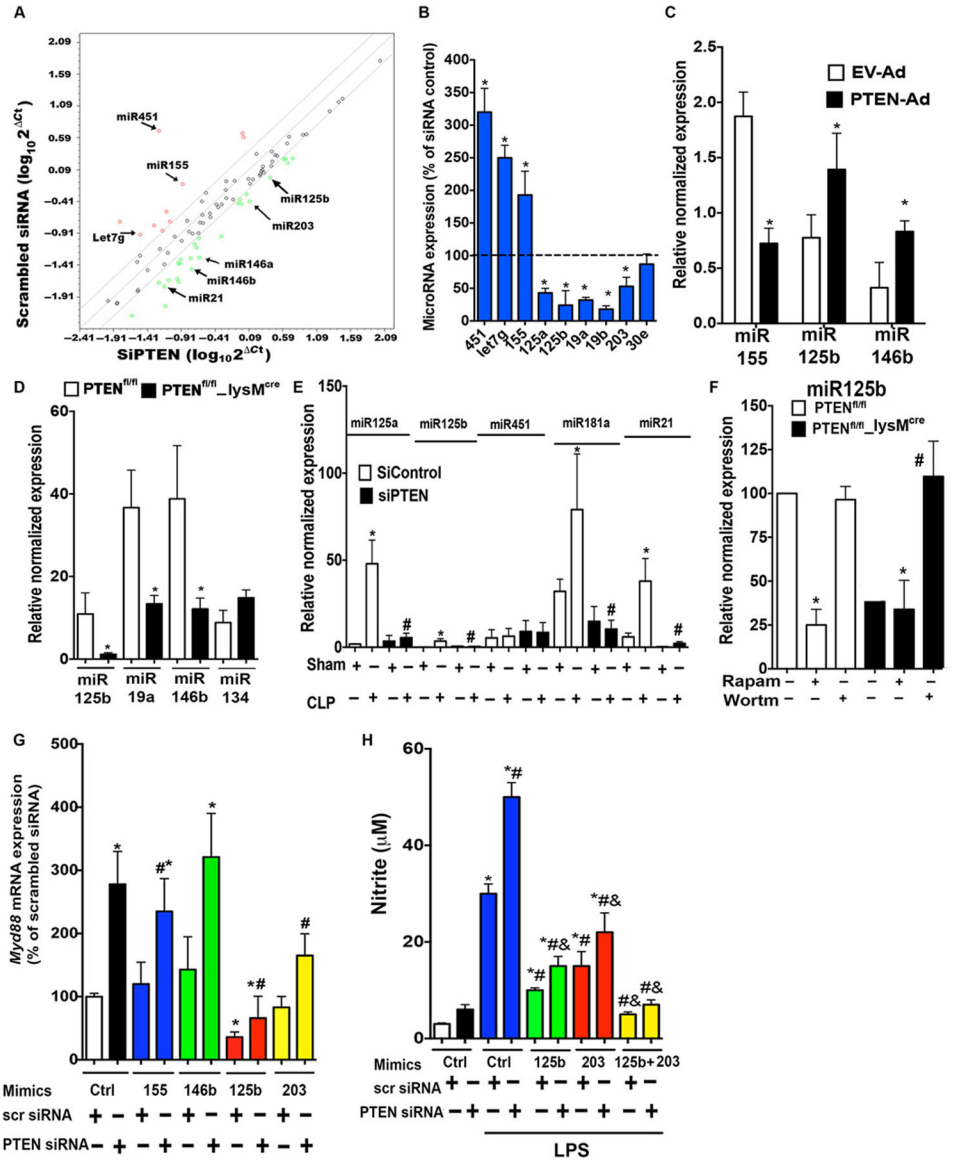

Figure 5. PTEN lipid phosphatase activity increases microRNA expression involved in *Myd88* expression and TLR activation in macrophages.

(A) Elicited macrophages were transfected with scramble siRNA control or PTEN siRNA. After 24 h, microRNAs were isolated and a microRNA-focused array was performed. (B) Elicited macrophages were transfected with PTEN siRNA as in (A), and expression of indicated microRNAs was determined by qPCR. Abundance relative to scrambled control siRNA expressed as mean ± SEM is shown. (C) Elicited macrophages were transduced with PTEN-expressing adenovirus or empty vector for 48 h and the expression of indicated microRNAs was determined by qPCR. Abundance relative to empty vector adenovirus (EV-Ad) expressed as mean ± SEM is shown. (D) Macrophages from PTEN$^{fl/fl}$ and PTEN$^{fl/fl}$_lysM^{cre} mice were isolated and the indicated microRNAs were detected by qPCR. Abundance relative to PTEN$^{fl/fl}$ macrophages expressed as mean ± SEM is shown. (E) CLP-induce sepsis was performed in PTEN$^{fl/fl}$ and PTEN$^{fl/fl}$_lysM^{cre} mice and microRNA abundance was measured in peritoneal cells 24 h post-CLP administration by qPCR.

Author Manuscript Author Manuscript Author Manuscript Author Manuscript

Abundance relative to control siRNA-treated Sham mice expressed as mean ± SEM is shown. (F) Macrophages from PTEN$^{fl/fl}$ and PTEN$^{fl/fl}$_lysM^{cre} mice were treated with the PI3K inhibitor wortmannin (Wortm) or the mTOR inhibitor rapamycin (Rapam) for 24 h, and expression of miR125b was determined by qPCR. Abundance relative to PTEN$^{fl/fl}$ macrophages treated with vehicle control expressed as mean ± SEM is shown. (G) Elicited peritoneal macrophages from wild-type mice were transfected with PTEN siRNA or scrambled siRNA as in (A) and with the indicated microRNA mimics for 24 h. *Myd88* mRNA abundance was determined by qPCR. Abundance relative to macrophages treated with scrambled control siRNA macrophages and the mimic control expressed as mean ± SEM is shown. (H) Macrophages from C57BL/6 mice were treated as in (G) and challenged with LPS for 24 h. Nitrite concentrations were determined in supernatants by Griess assay. Data are expressed as mean ± SEM from at least 5 mice/group repeated at three independent times and 1-way ANOVA followed by Bonferroni correction *$p<0.05$ compared to scramble siRNA control or PTEN$^{fl/fl}$; $^{\#}p<0.05$ LPS-stimulated PTEN siRNA compared to scramble siRNA control or PTEN$^{fl/fl}$ macrophages; $^{\&}p<0.05$ compared to microRNA mimic alone.

Author Manuscript Author Manuscript Author Manuscript Author Manuscript

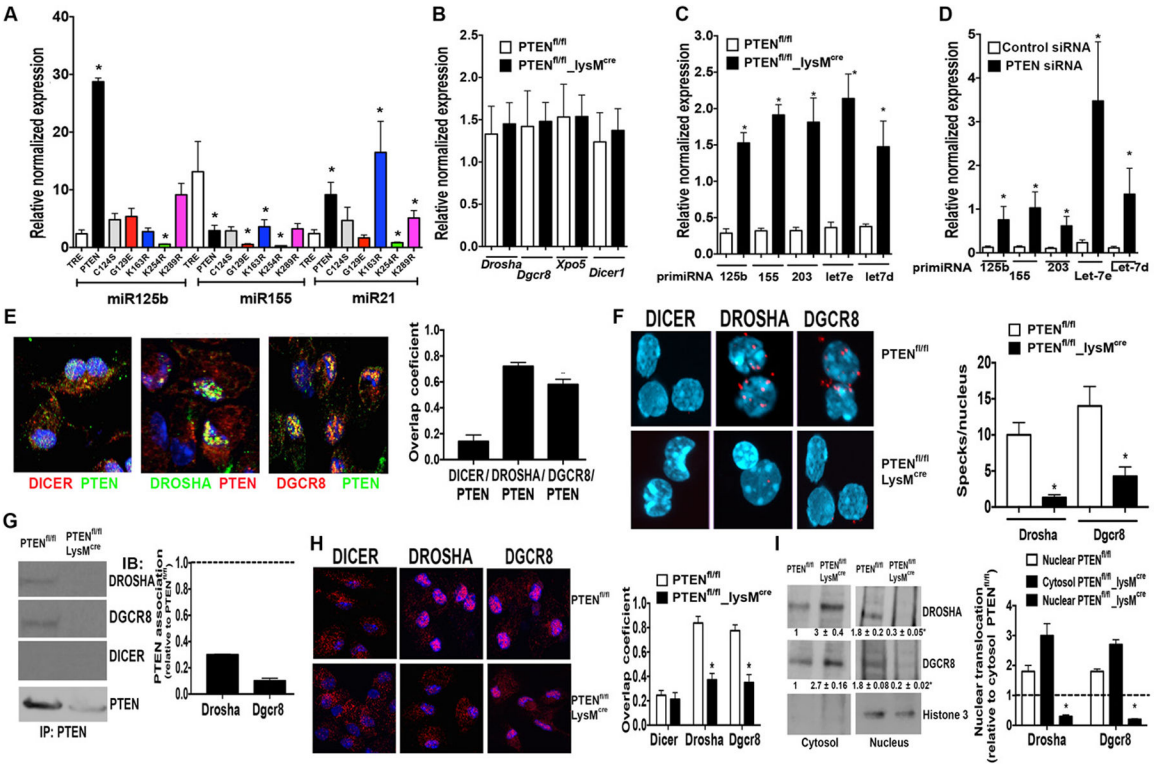

Figure 6. Nuclear PTEN drives microRNA processing.

(A) PTEN$^{-/-}$ MEFs were transduced with retrovirus-containing empty vector control (TRE) or the indicated wild-type or PTEN mutant constructs. Expression of the indicated microRNAs was determined by qPCR. Abundance relative to untransfected cells (TRE) expressed as mean ± SEM is shown (n=3 independent experiments and 1-way ANOVA followed by Bonferroni correction). (B) Macrophages from PTEN$^{fl/fl}$ and PTEN$^{fl/fl}$_lysM^{cre} mice were isolated and expression of *Drosha, Dgcr8, Xpo5*, and *Dicer 1* were determined by qPCR. Abundance relative to macrophages from PTEN$^{fl/fl}$ mice expressed as mean ± SEM is shown. (n = 4/group). (C) Primary microRNA expression in macrophages from PTEN$^{fl/fl}$ and PTEN$^{fl/fl}$_lysM^{cre} were determined by qPCR. Abundance relative to macrophages from PTEN$^{fl/fl}$ mice expressed as mean ± SEM is shown (n = 4/group). (D) Macrophages were treated with scrambled control or siPTEN and expression of primary microRNA was determined by qPCR. Abundance relative to macrophages treated with control siRNA expressed as mean ± SEM is shown (n=5/group). (E) Left - Macrophages from C57BL/6 were incubated with antibodies recognizing Drosha, Dgcr8, Dicer, or PTEN and visualized by confocal microscopy. Right – Overlap coefficient between PTEN/DICER, PTEN/Drosha and PTEN/Dgcr8. Data represent the mean ± SEM from 3 independent experiments, with ~100 cells analyzed in each experimental group. Blue indicates Dapi. Each field is representative of 100 examined (original magnification, ×400) per each of 3 independent experiments with the values from DICER/PTEN association set as 1. (F) Left - *In-situ* PLA of PTEN–Drosha or PTEN-Dgcr8 complexes in elicited macrophages from PTEN$^{fl/fl}$ and PTEN$^{fl/fl}$_lysM^{cre} mice. PLA complexes, red; nuclei, blue. Right - number of specks/ nucleus in at least 100 cells, expressed as the mean ± SEM from at least three independent experiments. (G) Right - PTEN was immunoprecipitated from total macrophage cell lysates

Author Manuscript Author Manuscript Author Manuscript Author Manuscript

from PTEN$^{fl/fl}$ and PTEN$^{fl/fl}$_lysM^{cre} mice and then samples were immunoblotted with antibodies against the indicated proteins. Left – Relative density of PTEN, DGCR8, Drosha, and DICER, determined by densitometry analysis and expressed as the mean ± SEM from 3 individual experiments, with the values of the PTEN$^{fl/fl}$ control group set as 1. (H) Left - Macrophages from PTEN$^{fl/fl}$ and PTEN$^{fl/fl}$_lysM^{cre} mice were incubated with antibodies recognizing Drosha, Dgcr8, or Dicer and visualized by confocal microcopy. Confocal images were taken with identical settings to allow comparison of staining intensities. Images are from one experiment, which are representative of 5 independent experiments. Right – Overlap coefficient between DAPI (nuclear blue) and Dgcr8, Drosha, or DICER (red). Data represent the mean ± SEM from 3 independent experiments, with ~100 cells analyzed in each experimental group with values from PTEN$^{fl/fl}$ set to 1. (I) Right - Nuclear and cytosolic fractions of macrophage cell lysates from PTEN$^{fl/fl}$ and PTEN$^{fl/fl}$_lysM^{cre} were isolated and immunoblotted with antibodies against the indicated proteins. Left - Relative density of DGCR8, Drosha, and Histone H3 determined by densitometry analysis and expressed as the mean ± SEM from 3 individual experiments, with the values of the cytosolic proteins from the PTEN$^{fl/fl}$ control group set as 1. Data are expressed as mean ± SEM from at least 5 mice/group. For all panels, *$p<0.05$ compared to empty vector, Control scrambled siRNA, or PTEN$^{fl/fl}$.